AD-A065 367 AIR FORCE INST OF TECH WRIGHT-PATTERSON AFB OHIO F/G 4/2
A TWO-DIMENSIONAL NUMERICAL MODEL OF DRY CONVECTION WITH THREE---ETC(U)
AUG 78 J C WEYMAN

UNCLASSIFIED AFIT-CI 79-74 NL

1 OF 1
ADA
065367

END
DATE
FILMED
4-79
DDC

AD A065367

LEVEL II (1) SC

TEXAS A&M UNIVERSITY
DEPARTMENT OF
METEOROLOGY

A TWO-DIMENSIONAL NUMERICAL MODEL OF DRY CONVECTION WITH THREE-DIMENSIONAL DYNAMICS

DDC FILE COPY

By

JAMES CHARLES WEYMAN

August 1978

DDC
RECEIVED
MAR 7 1979
E

DISTRIBUTION STATEMENT A
Approved for public release;
Distribution Unlimited

79 02 26 242

UNCLASSIFIED

SECURITY CLASSIFICATION OF THIS PAGE (When Data Entered)

REPORT DOCUMENTATION PAGE	READ INSTRUCTIONS BEFORE COMPLETING FORM
1. REPORT NUMBER: AFIT-CI 79-74	2. GOVT ACCESSION NO. (9) Master's thesis,	3. RECIPIENT'S CATALOG NUMBER
4. TITLE (and Subtitle): (6) A Two-Dimensional Numerical Model of Dry Convection with Three-Dimensional Dynamics.	5. TYPE OF REPORT & PERIOD COVERED: Thesis
	6. PERFORMING ORG. REPORT NUMBER
7. AUTHOR(s): James C. Weyman (10) James Charles Weyman	8. CONTRACT OR GRANT NUMBER(s): (12) 66p.
9. PERFORMING ORGANIZATION NAME AND ADDRESS: AFIT student at Texas A&M University	10. PROGRAM ELEMENT, PROJECT, TASK AREA & WORK UNIT NUMBERS
11. CONTROLLING OFFICE NAME AND ADDRESS: AFIT/CI WPAFB OH 45433	(11) 12. REPORT DATE: Aug 1978
	13. NUMBER OF PAGES: 58
14. MONITORING AGENCY NAME & ADDRESS (if different from Controlling Office)	15. SECURITY CLASS. (of this report): Unclassified
	15a. DECLASSIFICATION/DOWNGRADING SCHEDULE

16. DISTRIBUTION STATEMENT (of this Report)

Approved for Public Release, Distribution Unlimited

17. DISTRIBUTION STATEMENT (of the abstract entered in Block 20, if different from Report)

18. SUPPLEMENTARY NOTES

JOSEPH P. HIPPS, Major, USAF
Director of Information, AFIT
FEB 8 1979

19. KEY WORDS (Continue on reverse side if necessary and identify by block number)

20. ABSTRACT (Continue on reverse side if necessary and identify by block number)

012 200

DD FORM 1 JAN 73 1473 EDITION OF 1 NOV 65 IS OBSOLETE

UNCLASSIFIED

SECURITY CLASSIFICATION OF THIS PAGE (When Data Entered)

79-74T

A TWO-DIMENSIONAL NUMERICAL MODEL OF DRY CONVECTION WITH THREE-DIMENSIONAL DYNAMICS

A Thesis

by

JAMES CHARLES WEYMAN

Submitted to the Graduate College of
Texas A&M University
in partial fulfillment of the requirement for the degree of

MASTER OF SCIENCE

August 1978

ACCESSION for
NTIS White Section X
DDC Buff Section
UNANNOUNCED
JUSTIFICATION
BY
DISTRIBUTION/AVAILABILITY CODES
Dist. Avail. and/or SPECIAL
A

Major Subject: Meteorology

79 02 26 242

A TWO-DIMENSIONAL NUMERICAL MODEL OF DRY CONVECTION WITH THREE-DIMENSIONAL DYNAMICS

A Thesis

by

JAMES CHARLES WEYMAN

Approved as to style and content by:

_____
(Chairman of Committee)

_____
(Head of Department)

_____ _____
(Member) (Member)

August 1978

79-74T

ABSTRACT

A Two-Dimensional Numerical Model of Dry Convection With Three-Dimensional Dynamics. (August 1978)

James Charles Weyman, B.S., Grove City College

M.S.B.A., Metropolitan College

Chairman of Advisory Committee: Dr. Dusan Djuric

A numerical model for the study of dry, three-dimensional, small scale, atmospheric convection is presented for use with a two-dimensional grid in the vertical xz plane. All of the derivatives in the horizontal y dimension are derived through the assumptions of cyclostrophic balance, symmetry of circular eddies, and horizontal isotropy of derivatives. Variable eddy coefficients, proportional to the deformation field and the square of the grid interval, are used. Comparisons with a similar two-dimensional model shows the thermals in this pseudo three-dimensional model develop sooner and reach a larger maximum vertical velocity faster. These results are comparable to what other researchers of three-dimensional models have found. The economy of computation of this model will enable other investigators to make better use of limited computer facilities.

ACKNOWLEDGMENTS

I would like to express my gratitude to Dr. Dusan Djuric for the time, energy and encouragement he supplied throughout my studies at Texas A&M University. Through our many discussions I have gained a fuller knowledge and a better understanding of meteorology. Dr. Djuric's interest and enthusiasm in this research was an asset that I deeply appreciated. Since all good thesis must be looked at with a critical eye, I want to acknowledge Dr. K.C. Brundidge for his critical assessment of my work. Through his questions, he made me consider some things I had neglected or had quickly passed over. This I feel contributed to a more complete thesis. I also want to thank all of the meteorology professors at Texas A&M University for their assistance and teachings. Each of them has contributed in some way to my studies here.

My first and foremost acknowledgment has to be to my wife, Linda. She rejoiced with me on the days when things went well and consoled me when the outlook looked hopeless. My year and a half at Texas A&M and this thesis would not have been possible without her. Linda's many long hours and sacrifices will be remembered forever.

I wish to express my sincere gratitude to the Air Force Institute of Technology for sponsoring and financing my graduate program. I would also like to thank M. Riesener, Department of Meteorology, Freie Universitat, Berlin, for the vector derivation of (37).

Lastly, I want to acknowledge my parents, Mr. and Mrs. Edward Weyman, and my parents-in-law, Mr. and Mrs. Donald Wick, whose moral support is greatly appreciated.

TABLE OF CONTENTS

LIST OF FIGURES

1. INTRODUCTION

Numerical modelling is one of the promising ways to study the details of convective flow which cannot be practically observed. The models that have been tested thus far have differed greatly in the sophistication of the cloud physics and the numerical techniques employed. One of the earliest experiments was carried out in the mid-1950's at the Los Alamos Scientific Laboratory at the instigation of J. von Neumann. The results of this model were later published by Blair et al. (1959). Blair's model involved the simulated overturning of an unstably stratified, two-layer, incompressible fluid system. Then Lilly (1962) proposed a two-dimensional slab-symmetric model of buoyant convection. This model, which qualitatively and quantitatively resembled the convective thermals described by Scorer and Richards (1959), did not exhibit the shape preserving stage assumed in theoretical treatments and found by laboratory experiments. Lilly attributed this to the neglect of the effects of the eddies in the third dimension. Although Lilly met with limited success, his list of twelve areas to be studied further served as a guide for other researchers in the investigation of convective processes by numerical simulation.

Using many of Lilly's suggestions, a number of different models were investigated in the 1960's. Ogura (1962) used an axially symmetric model to simulate a buoyant mass of fluid embedded in an ambient

---

The format and style of this thesis follow those of the Journal of Atmospheric Sciences.

fluid of uniform density. The results from Ogura's model exhibited the shape preserving stage that Lilly's experiment could not. However, Ogura's model was unable to handle wind shear. Ogura and Charney (1960) developed a two-dimensional slab-symmetric model to simulate a squall line. The serious disadvantage in their studies was that the resulting downward motion began very close to the upward thermal, thereby cutting off the supply of warm air necessary for the upward motion. The thermal was greatly weakened after this occurred. Squires and Turner (1962) used a one-dimensional model to study cumulonimbus updrafts. They allowed for the entraining of environmental air by assuming the inflow velocity was proportional to the upward velocity of the plume. They also allowed for the incorporation of latent heat of freezing by assuming the proportion of ice to total condensed material varied linearly with temperature. Squires' and Turner's model yielded results which seemed reasonably consistent with observations, especially in regard to cloud shape. However, since the model was one dimensional, it could not adequately represent the horizontal variations of conditions within the cloud. Orville (1964, 1965) used a two-dimensional slab-symmetric model to simulate mountain upslope winds. Although his results were similar to the observations available, he believed that the two- rather than the three-dimensional treatment may be the largest drawback. The reason was that the downward vertical motion and the energy budget were not sufficiently satisfied in the two-dimensional model. Orville (1968) used an improved two-dimensional slab-symmetric model to simulate the development of cumulus clouds over a mountain.

Although Orville's results were an improvement over his 1964 and 1965 work, he still specified his major problem was the missing third dimension.

With the advent of larger and faster computers during the late 1960's and early 1970's, it became possible to construct three-dimensional models. Deardorff (1970) was one of the first to model in three dimensions when he investigated three-dimensional turbulent channel flow at large Reynolds numbers. Although the resolution was modest at first (24 X 14 X 20 grid points), the cascade of energy from large scales to smaller scales, which scarcely occurred in two dimensions, was very discernable in three dimensions. This turbulence model was extended by Deardorff (1972) to the study of neutral and unstable planetary boundary layers using a grid of 40 X 40 X 20 points. This model was further increased to 40 X 40 X 40 points by Deardorff (1973) to study the use of subgrid transport equations in a three-dimensional model of atmospheric turbulence. Following Deardorff's work, a number of other investigators began using three-dimensional models. Fox (1972) used a 12 X 12 X 54 grid in a three-dimensional model to simulate a three-dimensional thermal. Although Fox felt that three-dimensional simulation was a great improvement over two-dimensional work, he stated that turbulent thermals could not be completely simulated without more powerful computers and vastly more computer time. Other three-dimensional models have been proposed by Steiner (1973), Wilhelmson (1974), Miller and Pearce (1974), and Schlesinger (1975). Schlesinger stated that the number of three-dimensional models has not been larger mainly because they

demand large amounts of computing storage and expenditures if adequate resolution is to be achieved.

From the above discussion, disadvantages of the present one-, two-, and three-dimensional models have been shown to limit the complete study of convective processes. An alternative model was proposed by Deardorff (1965). He described a pseudo three-dimensional model which allowed the third dimension to be simulated while the computations were done in two dimensions. This method would combine the advantages of the two- and three-dimensional models. Due to poor results when treating convection at small Prandtl numbers and to the significant advancement in computers during the late 1960's (Deardorff, personal communication), Deardorff never continued this research, but instead began his three-dimensional model. However, Gruneberg (1975) decided to continue this research of a pseudo three-dimensional model because of the limitations, suggested by Schlesinger (1975) and Fox (1972), of three-dimensional models to most researchers. Although Gruneberg used Deardorff's idea of a pseudo three-dimensional model, his physical and statistical assumptions for the simulated third dimension (y) were different. Gruneberg's model produced results which were only slightly different than conventional two-dimensional models. He contributed these results to his treatment of the pressure force. In Gruneberg's model, the first derivative of pressure with respect to y was a statistical parameter, and not based on the properties of the flow. The second derivative of pressure with respect to y was not included. Jenkins (1976) working with Gruneberg's model, remedied this situation.

The statement for the first derivative of pressure with respect to y was based on the assumption that for convective processes, the magnitude of the local time derivative is much smaller than the centrifugal force. Therefore, the cyclostrophic approximation was used. The inclusion of the second derivative of pressure was based on the assumption that the pressure distribution in axially symmetrical vortices was also axially symmetric.

Although Jenkins' results were an improvement over Gruneberg's findings when compared to three-dimensional models, serious problems still existed. Numerical instability occurred after 15 min of simulated time which severely limited the usefulness of the results. Also, large unexplained gradients in the vertical motion and potential temperature fields developed near the bottom of the layer under consideration. At present, no one has investigated these limiting features of this potentially valuable model.

It is the purpose of this research, therefore, to determine if the two-dimensional assumptions may be replaced by pseudo three-dimensional assumptions in a numerical model to produce thermal convection in better agreement with true three-dimensional models.

2. GOVERNING EQUATIONS

The basic equations to be used in this model are the horizontal and vertical equations of motion, the thermal diffusion equation, and the continuity equation. These equations are for a dry, incompressible atmosphere.

$$u_t = -uu_x - vu_y - wu_z - p_x + F_1 \tag{1}$$

$$v_t = -uv_x - vv_y - wv_z - p_y + F_2 \tag{2}$$

$$w_t = -uw_x - vw_y - ww_z - p_z + F_3 + b \tag{3}$$

$$b_t = -ub_x - vb_y - wb_z + F_4 \tag{4}$$

$$0 = u_x + v_y + w_z \tag{5}$$

The variables u, v and w are the components of motion in the x, y and z directions, respectively. The use of subscripts refers to the partial derivative of the subscripted variable with respect to the subscript. The variable p is the ratio of the pressure deviation from a hydrostatic basic state to the density, b is buoyancy, F_1, F_2 and F_3 are the friction terms and F_4 is the thermal diffusion term. The variables u, v, w, b and p are averaged values over an elemental grid volume. The friction terms, the thermal diffusion terms and buoyancy are defined as follows:

$$F_1 = \nabla \cdot (K_m \nabla u) \tag{6}$$

$$F_2 = \nabla \cdot (K_m \nabla v) \tag{7}$$

$$F_3 = \nabla \cdot (K_m \nabla w) \tag{8}$$

$$F_4 = \nabla \cdot (K_h \nabla b) \tag{9}$$

$$b = g\left(\frac{\theta'}{\theta}\right) \tag{10}$$

The variable g is the acceleration due to gravity, θ is a constant basic potential temperature, and θ' is the deviation from the horizontally (x direction) averaged potential temperature. The explanation of this choice for the formulation of buoyancy will be presented in Section 3. K_m and K_h are the eddy viscosity and thermal diffusivity coefficients, respectively. These coefficients are allowed to vary with time and space, and are computed locally by

$$K_m = (c\Delta)^2 \left[1/2\left(\frac{\partial u_i}{\partial x_j} + \frac{\partial u_j}{\partial x_i}\right) \left(\frac{\partial u_i}{\partial x_j} + \frac{\partial u_j}{\partial x_i}\right) \right]^{1/2} \qquad (11)$$

$$K_h = 3.0K_m \qquad (12)$$

The quantity Δ is the representative grid interval, c is a dimensionless constant, and the indexes i and j have values of 1, 2 and 3. This formulation, although at first was used for general circulation models (Leith, 1965, Mintz, 1965, and others), was shown to be applicable when the inertial subrange exists on scales encompassing the grid interval by Lilly (1967), and Leith (1968), and Deardorff (1970). The formulation of K_m and K_h will be discussed more fully in Section 3.

In order to evaluate the pressure field, a balance equation for pressure is formed. This is done by taking the divergence of (1)-(3) and by making use of (5). The result is

$$p_{xx} + p_{yy} + p_{zz} = \text{div}\left[-\underset{\sim}{A}(\underset{\sim}{V}) + \underset{\sim}{F} + b\underset{\sim}{k}\right] \qquad (13)$$

where $\underset{\sim}{A}(\underset{\sim}{V})$ represents the advective terms in (1)-(3) and $\underset{\sim}{k}$ is the ver-

tical unit vector. Eq. (13) is a Poisson equation of the form

$$\underset{\sim}{\nabla}^2 p = F$$

which can be solved directly by the use of a Fourier transform, in which the two-dimension problem can be reduced to a set of one-dimensional problems.

3. PSEUDO THREE-DIMENSIONAL ASSUMPTIONS

In this model all of the computations involving the various terms are done in the vertical x-z plane. Therefore, all of the y derivatives in the basic equations must be determined using other equations or model assumptions. Eq. (5), the continuity equation for an incompressible atmosphere was used once in the derivation of (13), the balance equation for pressure, but it may be used once more in order to eliminate v_y. When (5) is combined with (2), the resulting equation is

$$v_t = -uv_x + v(u_x + w_z) - wv_z - p_y + F_2 \tag{14}$$

which is used in the basic equations instead of (2).

The second derivative of v with respect to y is also needed in the basic equations. When the divergence of the advection terms in (13) is taken, one obtains a term

$$-(vv_y)_y = -v_y v_y - vv_{yy}.$$

The continuity equation is used again to eliminate v_{yy}. If the partial derivative of (5) with respect to y is taken, the result is

$$v_{yy} = -(u_x)_y - (w_z)_y.$$

Then if the various functions are continuous, the order of differentiation may be reversed and one arrives at

$$v_{yy} = -(u_y)_x - (w_y)_z .$$

This can now be used in (13).

The derivatives u_y, w_y, and b_y are treated as new variables for which new equations are needed. These new equations are obtained by taking the derivatives of (1), (3), and (4) with respect to y. Again assuming that the various functions are continuous, the order of differentiation is reversed. The resulting equations are

$$(u_y)_t = -u(\underline{u_y})_x - v(u_y)_y - w(\underline{u_y})_z - u_x\underline{u_y} - \underline{u_y}v_y - \underline{w_y}u_z - (p_y)_x + (F_1)_y \quad (15a)$$

$$(w_y)_t = -u(\underline{w_y})_x - v(w_y)_y - w(\underline{w_y})_z - w_x\underline{u_y} - w_y v_y - \underline{w_y}w_z - (p_y)_z + (F_2)_y \quad (15b)$$

$$(b_y)_t = -u(\underline{b_y})_x - v(b_y)_y - w(\underline{b_y})_z - b_x\underline{u_y} - \underline{b_y}v_y - \underline{w_y}b_z + (F_4)_y \quad (15c)$$

In order to find the underlined y derivatives in these equations, the assumptions of horizontal homogeneity and horizontal isotropy in free convection are made. These assumptions mean that the turbulence has quantitatively the same structure in the two horizontal directions of the flow field (horizontal homogeneity) and that the average value of any function of the velocity components, defined in relation to a given set of horizontal axes, is unaltered if the horizontal axes of reference are rotated in any manner (horizontal isotropy). Therefore, by making the assumption that the flow is isotropic one obtains

$$\overline{(u_y)^2} = \overline{(v_x)^2} \qquad \overline{(w_x)^2} = \overline{(w_y)^2}$$

and

$$\overline{(b_y)^2} = \overline{(b_x)^2} \quad (16)$$

(See Taylor, 1935)

The Glossary of Meteorology (1959) says that although atmospheric turbulence is generally non-isotropic, isotropic turbulence forms the basis of most theoretical analysis of turbulent flow. Hinze (1975) states that a knowledge of the characteristics of isotropic turbulence, notwithstanding its hypothetical character, may still form a fundamental basis for the study of actual, non-isotropic turbulent flows. He continues by saying that many features of isotropic turbulence apply to phenomena in actual turbulence. In numerical work, Deardorff (1965) uses the horizontally homogeneous and isotropic turbulence assumption in a similar manner to what has been done in this research. Therefore, these two assumptions are not expected to be too restrictive.

After the values of u_y, w_y, and b_y are determined initially at the first time step or are found at the beginning of each succeeding time step by the left-hand side of (15a), (15b), and (15c), these values are adjusted so that the isotropic conditions are satisfied. This is done by correcting u_y, w_y, and b_y in the following manner:

$$u_{y(new)} = u_y \left[\frac{\sum (v_x)^2}{\sum (u_y)^2}\right]^{1/2} \tag{17}$$

$$w_{y(new)} = w_y \left[\frac{\sum (w_x)^2}{\sum (w_y)^2}\right]^{1/2} \tag{18}$$

$$b_{y(new)} = b_y \left[\frac{\sum (b_x)^2}{\sum (b_y)^2}\right]^{1/2} \tag{19}$$

The summations that are used in (17) - (19) are over a horizontal row of grid points in the x direction. These equations alter u_y, w_y, and b_y in such an amount that (16) is satisfied.

However, if horizontal isotropy is assumed, Deardorff (1965) suggests that there should be constraints upon the lateral (y) advection so as not to affect the mean values. This is due to the fact that the failure to constrain the lateral advection terms could cause spurious instability. This will be discussed more fully later.

The reason for these constraints arises in the following manner. The equation of continuity which has been multiplied by -b and the advective terms of the thermal diffusion equation are

$$0 = -b\,(u_x + v_y + w_z) \tag{21}$$

$$b_t = -ub_x - vb_y - wb_z \quad , \tag{22}$$

respectively. If these two equations are added together, the flux form,

$$b_t = -(ub)_x - (vb)_y - (wb)_z \quad , \tag{23}$$

is obtained. If this were a true three-dimensional model, then the average at each level over the horizontal plane (x-y) would be

$$\overline{b_t}^{xy} = \overline{-(ub)_x}^{xy} \; \overline{-(vb)_y}^{xy} \; \overline{-(wb)_z}^{xy} \quad . \tag{24}$$

With cyclic boundary conditions in the x and y directions,

$$\overline{\overline{(ub)_x}^{xy}} = 0$$

and

$$\overline{\overline{(vb)_y}^{xy}} = 0 \quad .$$

Therefore,

$$\overline{\overline{b_t}^{xy}} = \overline{\overline{-(wb)_z}^{xy}} \quad .$$

In this research all of the variables are defined only on the x-z plane, and an average over the x-y plane is not possible. However, an average of (23) can be taken in the x direction. This equation is

$$\overline{\overline{b_t}^{x}} = \overline{\overline{-(ub)_x}^{x}}\ \overline{\overline{-(vb)_y}^{x}}\ \overline{\overline{-(wb)_z}^{x}} \quad . \tag{25}$$

Here

$$\overline{\overline{(ub)_x}^{x}} = 0 \ , \tag{26}$$

because cyclic conditions are assumed in the x direction. Since the isotropic assumption assumes similar statistical properties on the average in the x and y directions, it is necessary therefore to make

$$\overline{\overline{(vb)_y}^{x}} = 0 \quad . \tag{27}$$

This requirement is analogous to the three-dimensional case and assures that nothing different is going on in the y direction, on the average, than in the x direction. Although it is true that within a single x-z vertical slice of real three-dimensional motion one does not expect (27) to hold precisely unless the slice extends very far in the x direction, this condition should not be violated significantly or systematically. Since (26) is exactly zero, it is only consistent that (27) be made to hold as exactly as possible.

Nonlinear computational instability arises because of the nonlinear interaction between different wave modes in the numerical evaluation of the advection terms. Lilly (1965) points out that to insure stability in the absence of net boundary fluxes the finite difference form of the advection terms should conserve linear and quadratic quantities. There are no net fluxes in the x and y direction for the true three-dimensional case (24) shown before, because cyclic conditions are assumed in x and y. In this case the mean values are correctly conserved in the horizontal, since the averaged horizontal flux terms in (24) are zero. For the pseudo three-dimensional model used in this research, there are no net fluxes in the x direction because of cyclic conditions, and the x direction flux terms average to zero conserving the mean values. The y direction flux terms should also conserve the mean values due to isotropic considerations and in analogy to the three-dimensional case. There is no way to ensure this requirement unless (27) is satisfied. This condition also avoids the spurious instability mentioned by

Deardorff (1965). A similar argument can be made for the quadratic terms, and this will be covered later.

Therefore from (27), the constraint upon the lateral advection so as not to affect the mean value of b is

$$\overline{vb_y}^x = \overline{-bv_y}^x \quad . \tag{28a}$$

Similar constraints upon the lateral advection so as not to affect the mean values of u, w, u_y, w_y, and b_y can be developed.

This is accomplished by multiplying the continuity equation first by u to receive the first equation, then by w to get the second, by u_y for the third, by w_y for the fourth, and by b_y for the fifth. Then the first equation can be added to the advective terms of (1), the second equation can be added to the advective terms of (3), and the third, fourth, and fifth can be added respectively to the advective terms of (15a), (15b) and (15c). An average in the x direction of the five resulting flux form equations is taken. Because cyclic conditions are assumed in the x direction, and the isotropic assumption assumes similar statistical properties on the average in the x and y directions, one obtains

$$\overline{vu_y}^x = \overline{-uv_y}^x \qquad \overline{vu_{yy}}^x = \overline{-u_y v_y}^x$$

$$\overline{vw_y}^x = \overline{-wv_y}^x \qquad \overline{vw_{yy}}^x = \overline{-w_y v_y}^x$$

$$\overline{vb_{yy}}^x = \overline{-b_y v_y}^x \quad . \tag{28b}$$

Another important constraint is that for p_y. If the continuity equation is multiplied by -p and then added to the pressure force terms of the kinetic energy equation, the result is a flux form equation. A spatial average in the x direction of the resulting equation is taken. Due to isotropy, the constraint for p_y is given by

$$\overline{vp_y}^x = \overline{-pv_y}^x \quad . \tag{28c}$$

This constraint is very important if p_y in (14) is to properly simulate the transfer of kinetic energy (generated by buoyancy) from the vertical component into the horizontal component of motion.

In addition to the constraints upon the lateral advection so as not to affect the means, Deardorff (1965) suggests that there should also be constraints upon the lateral advection so as not to affect the mean squared or quadratic values. Even if the assumptions connected with the lateral advection terms leave the x mean unchanged, these advection terms could spuriously alter the mean squared values. The formulation of these constraints is done in the following manner. If (21) is multiplied by b and (22) by 2b and the resulting equations are added together and averaged, one obtains

$$\overline{(b^2)_t}^x = \overline{-(ub^2)_x}^x \quad \overline{-(vb^2)_y}^x \quad \overline{-(wb^2)_z}^x \quad . \tag{29}$$

Since the first term on the right-hand side of (29) equals zero exactly due to cyclic conditions in x, the second term should also

equal zero exactly. This is necessary because of the horizontally isotropic and homogeneity assumptions as pointed out before and to avoid the spurious instability as discussed previously. Therefore the constraint upon the lateral advection so as not to affect the mean of b^2 is

$$\overline{v(b^2)_y}^x = \overline{-b^2 v_y}^x \quad . \tag{30a}$$

Constraints upon the lateral advection so as not to affect the mean of u^2, w^2, $(u_y)^2$, $(w_y)^2$, and $(b_y)^2$ can be developed. These constraints are

$$\overline{v(u^2)_y}^x = \overline{-u^2 v_y}^x \qquad \overline{v\ (u^2)_y\ _y}^x = \overline{-(u_y)^2 v_y}^x$$

$$\overline{v(w^2)_y}^x = \overline{-w^2 v_y}^x \qquad \overline{v\ (w^2)_y\ _y}^x = \overline{-(w_y)^2 v_y}^x$$

$$\overline{v\ (b^2)_y\ _y}^x = \overline{-(b_y)^2 v_y}^x \tag{30b}$$

The values of u_y, w_y, and b_y, given in the first time step by the initial conditions or after that found for a new step by the left-hand side of (15a), (15b), and (15c), were first adjusted for the isotropic conditions by (17) - (19). Now these values must be corrected for the constraints in (28a), (28b), (30a), and (30b). This is done in the following manner.

Since v_y is determined from the continuity equation, v_y can be used to calculate

$$\overline{-bv_y}^x \qquad \text{and} \qquad \overline{-b^2 v_y}^x \quad .$$

Then, b_y can be corrected to satisfy the equations

$$\overline{vb_y}^x = \overline{-bv_y}^x \quad \text{and} \quad \overline{v(b^2)_y}^x \text{ or } \overline{2vbb_y}^x = \overline{-b^2 v_y}^x \quad . \tag{31}$$

The necessary corrections for b_y will be proportional to v and 2vb,

$$b_{y(new)} = b_y + k_1 v$$

$$b_{y(new)} = b_y + k_2 2vb \quad , \tag{32}$$

respectively, where k_1 and k_2 are the correction factors. These corrections are chosen, because it cannot be expected that these averages,

$$\overline{vb_y}^x \qquad \text{and} \qquad \overline{2vbb_y}^x \quad ,$$

will tend to the correct values unless one of the members (b_y) is corrected by a quantity ($k_1 v$ or $k_2 2vb$) which is proportional to the other member (v or 2vb). If (32) is substituted into (31), the result is

$$\overline{vb_{y(new)}}^x = \overline{v(b_y + k_1 v)}^x = \overline{-bv_y}^x \quad , \; k_1 = \frac{\overline{-bv_y}^x \; \overline{-vb_y}^x}{\overline{v^2}^x}$$

and

$$\overline{2vbb_{y(new)}}^{x} = \overline{2vb(b_y + k_2 2vb)}^{x} = \overline{-b^2 v_y}^{x}, \quad k_2 = \frac{\overline{-b^2 v_y}^{x} - \overline{2vbb_y}^{x}}{\overline{4v^2 b^2}^{x}}.$$

An overrelaxed iteration procedure is used to correct b_y, so that a $b_{y(new)}$ is found that will satisfy both equations in (31). Similar procedures can be programmed to satisfy all of the constraints in (28a), (28b), (30a), and (30b). Now that u_y, w_y, and b_y have been adjusted for the isotropic conditions (17-19) and corrected for the constraints in (28a), (28b), (30a), and (30b), they may be used in the right-hand side of (15a), (15b), and (15c) to predict new values in time of u_y, w_y, and b_y respectively. Also in (15a), (15b), and (15c), values of u_{yy}, w_{yy}, and b_{yy} are needed. As a result of enforcing the constraints of (28a), (28b), (30a), and (30b), one is provided with a method to determine these.

Eqs. (11) and (12), the formulation for the eddy coefficients used in this model, were first proposed by Smagorinsky (1963). In this formulation the eddy coefficients are assumed proportional to the magnitude of the velocity deformation field and to the square of the grid interval. Lilly (1967) showed that this treatment is consistent with the existence of a three-dimensional inertial subrange on scales comparable to and less than the grid interval. In the same paper, Lilly (1967) also estimated the value of c in (11) to be $0.23\alpha^{-3/4}$ where α is the approximate value of the Kolmogorov

inertial-subrange constant. Deardorff (1971) shows for $\alpha = 1.41$, an averaged value obtained from Pond et al. (1963), Lilly's formulation give c = 0.176. However, Lilly (1966) found that when the deformation field is obtained from finite differences across single grid intervals, c increases 25% giving c = 0.22. Deardorff (1970) found a similar value, 0.21, for the case of an unstably stratified planetary boundary layer. Due to the staggered grid arrangement in this research, it is necessary to take finite differences across two grid intervals for about 50% of the terms in the deformation equation. Therefore it is found that a value for c of 0.25 or 13% larger than Lilly's value achieved the best results. Deardorff (1972) improved this formulation when he discovered that the ratio of K_h/K_m had to be between two and three to avoid excessive intensities in the temperature spectrum at large wave numbers. A value of three for this ratio is used in this research.

In this treatment of the eddy coefficients and the diffusion terms, an assumption is needed for the y derivatives so that they may be included in this pseudo three-dimensional model. For example, in (1) F_1 is defined as

$$F_1 = (K_m u_x)_x + (K_m u_y)_y + (K_m u_z)_z \quad .$$

From previous assumptions u_y can be determined, but the quantity $(K_m u_y)_y$ cannot. For this term it is assumed that

$$(K_m u_y)_y = (K_m u_y)_x$$

at each point. Since horizontal homogeneity is assumed, $(K_m u)_{yy}$ should vary in space and time in a manner consistent with $(K_m u)_x$. This assumption fulfills this requirement, whereas the other two possibilities

$$(K_m u)_{yy} = 0 \quad , \quad (K_m u)_y = \text{constant in y direction}$$

and

$$(K_m u)_{yy} = K_m u_{yy}, \quad K_m = \text{constant in y direction}$$

do not.

Another y derivative that must be determined is the first derivative of pressure with respect to y. This is needed in (14) to calculate v_t. For the convection process under consideration, the magnitudes of the local time derivative and the coriolis force are much smaller than the centrifugal force. Hence, the cyclostrophic approximation, where the centrifugal force balances the pressure force, can be used to calculate p_y. The cyclostrophic balance can be stated in the form

$$-\nabla p = \underset{\sim}{C} V^2 \tag{33}$$

where $\underset{\sim}{C}$ is the three-dimensional streamline curvature vector, and V is the magnitude of the three-dimensional wind vector. The curvature vector points toward the center of curvature with a magnitude of 1/r. It is helpful at this point to introduce a natural coordinate system. The direction of the coordinates, s, n, and z, in this system are defined by unit vectors $\underset{\sim}{t}$, $\underset{\sim}{n}$, and $\underset{\sim}{k}$, respectively. The unit

vector $\underset{\sim}{t}$ is parallel to the flow at each point, $\underset{\sim}{n}$ is normal to the flow and is directed toward the center of curvature, and $\underset{\sim}{k}$ is normal to the flow and equals $\underset{\sim}{t} \times \underset{\sim}{n}$. In this system the velocity may be written as

$$\underset{\sim}{V} = V\underset{\sim}{t} \qquad \text{or} \qquad \underset{\sim}{t} = \underset{\sim}{V}/V \ .$$

The rate of change of $\underset{\sim}{t}$ following the motion may be derived from geometrical consideration in a manner similar to that used by Holton (1972) to find $d\underset{\sim}{V}/dt$.

Recalling that $\left|\underset{\sim}{t}\right| = 1$, then

$$\delta\theta = \delta s/R = \left|\delta\underset{\sim}{t}\right| / \left|\underset{\sim}{t}\right| = \left|\delta\underset{\sim}{t}\right| = \left|\delta\underset{\sim}{V}/V\right| \text{ and } \left(\left|\delta\underset{\sim}{V}/V\right|\right)/\delta s = 1/R \qquad (34)$$

can be shown to be true from Fig. 1.

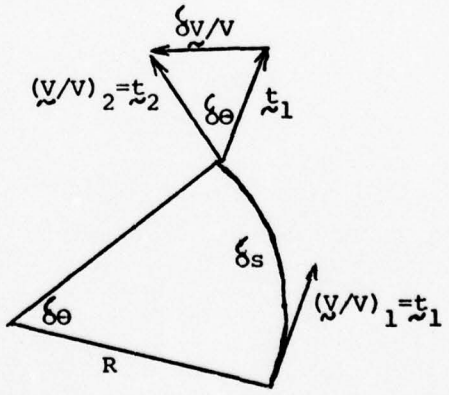

Fig. 1. A small segment of flow in a natural coordinate system (After Holton, 1972).

By noting that $\delta\underset{\sim}{t}$ is directed parallel to $\underset{\sim}{n}$ in the limit as $\delta s \to 0$, the equation

$$\frac{\partial}{\partial s}\left(\underset{\sim}{V}/V\right) = \underset{\sim}{n}/R = \underset{\sim}{C} \tag{35}$$

is obtained from (34). After performing the necessary differentiation, the curvature vector is given by

$$\underset{\sim}{C} = \frac{\partial}{\partial s}\left(\underset{\sim}{V}/V\right) = \frac{1}{V^2}\left[V\frac{\partial \underset{\sim}{V}}{\partial s} - \underset{\sim}{V}\frac{\partial V}{\partial s}\right]. \tag{36}$$

The derivatives along the streamline direction, s, are obtained by the use of the chain rule and by the use of the following relations.

$$\frac{\partial \underset{\sim}{V}}{\partial s} = \frac{\partial \underset{\sim}{V}}{\partial \underset{\sim}{r}} \cdot \frac{\partial \underset{\sim}{r}}{\partial s} \qquad \underset{\sim}{r} = s\left(\underset{\sim}{V}/V\right)$$

$$\frac{\partial V}{\partial s} = \frac{\partial V}{\partial \underset{\sim}{r}} \cdot \frac{\partial \underset{\sim}{r}}{\partial s} \qquad \frac{\partial \underset{\sim}{r}}{\partial s} = \underset{\sim}{V}/V$$

In these relations, $\underset{\sim}{r}$ is the cartesian position vector, and $\frac{\partial \underset{\sim}{V}}{\partial \underset{\sim}{r}}$ is a dyadic tensor. Eq. (36) now becomes

$$\underset{\sim}{C} = \frac{1}{V^2}\left\{V\left[\left(\underset{\sim}{V}/V\right) \cdot \frac{\partial \underset{\sim}{V}}{\partial \underset{\sim}{r}}\right] - \underset{\sim}{V}\left[\left(\underset{\sim}{V}/V\right) \cdot \left(\frac{\partial V}{\partial \underset{\sim}{r}}\right)\right]\right\},$$

or

$$\underset{\sim}{C} = \frac{1}{V^2}\left\{\underset{\sim}{V} \cdot \underset{\sim}{\nabla}\underset{\sim}{V} - \underset{\sim}{V}\left[\left(\underset{\sim}{V}/V\right) \cdot \underset{\sim}{\nabla} V\right]\right\}. \tag{37}$$

To resolve (37) into a more workable form, the approach of Riesener (personal communication) is shown below. It can be shown that

$$\frac{1}{V}\,\underset{\sim}{\nabla}\,\underset{\sim}{V}\cdot\underset{\sim}{V}=\frac{1}{V}\,\underset{\sim}{\nabla}\,(\underset{\sim}{V}\cdot\underset{\sim}{V})-\frac{1}{V}\,\nabla\underset{\sim}{V}\cdot\underset{\sim}{V}$$

and it follows that

$$\frac{1}{V}\,\underset{\sim}{\nabla}\,\underset{\sim}{V}\cdot\underset{\sim}{V}=\frac{1}{2V}\,\underset{\sim}{\nabla}\,(V^2)=\underset{\sim}{\nabla}\,V \quad . \tag{38}$$

If (38) is substituted into (37),

$$\underset{\sim}{C}=\frac{1}{V^2}\left[\underset{\sim}{V}\cdot\underset{\sim}{\nabla}\,\underset{\sim}{V}-\frac{1}{V^2}\,\underset{\sim}{V}\,\underset{\sim}{V}\cdot\underset{\sim}{\nabla}\,\underset{\sim}{V}\cdot\underset{\sim}{V}\right] \tag{39}$$

is obtained. Since $\underset{\sim}{V}\cdot\underset{\sim}{V}/V^2 = 1$, the first right-hand term of (39) can be multiplied by this to produce

$$\underset{\sim}{C}=\frac{1}{V^2}\left[(\underset{\sim}{V}\cdot\underset{\sim}{\nabla}\,\underset{\sim}{V})\,\frac{\underset{\sim}{V}\cdot\underset{\sim}{V}}{V^2}-\frac{1}{V^2}\,\underset{\sim}{V}\,\underset{\sim}{V}\cdot\underset{\sim}{\nabla}\,\underset{\sim}{V}\cdot\underset{\sim}{V}\right]$$

or

$$\underset{\sim}{C}=\frac{1}{V^4}\left[(\underset{\sim}{V}\cdot\underset{\sim}{\nabla}\,\underset{\sim}{V})\,\underset{\sim}{V}-\underset{\sim}{V}\,\underset{\sim}{V}\cdot\underset{\sim}{\nabla}\,\underset{\sim}{V}\right]\cdot\underset{\sim}{V} \quad . \tag{40}$$

If $\underset{\sim}{A}(\underset{\sim}{V})$ is defined as $\underset{\sim}{V}\cdot\underset{\sim}{\nabla}\,\underset{\sim}{V}=\underset{\sim}{A}(\underset{\sim}{V})$, where $\underset{\sim}{A}(\underset{\sim}{V})$ represents the advection terms, (40) becomes

$$\underset{\sim}{C}=\frac{1}{V^4}\left[\underset{\sim}{A}\,(\underset{\sim}{V})\,\underset{\sim}{V}-\underset{\sim}{V}\,\underset{\sim}{A}\,(\underset{\sim}{V})\right]\cdot\underset{\sim}{V} \quad . \tag{41}$$

With the aid of the vector identity, $(\underset{\sim}{a}\times\underset{\sim}{b})\times\underset{\sim}{c}=(\underset{\sim}{b}\underset{\sim}{a}-\underset{\sim}{a}\underset{\sim}{b})\cdot\underset{\sim}{c}$, an equation for $\underset{\sim}{C}$ is found from (41) such that

$$\underset{\sim}{C}=\frac{1}{V^4}\left[\underset{\sim}{V}\times\underset{\sim}{A}\,(\underset{\sim}{V})\right]\times\underset{\sim}{V} \quad . \tag{42}$$

With the aid of (33) and (42), the value of p_y may be specified as

$$-p_y = V^2 C_2 = \frac{1}{V^2}\left[u(uA_2 - vA_1) + w(wA_2 - vA_3)\right] , \qquad (43)$$

and this value can be used in (14).

The last y derivative need for the basic equations is p_{yy}. The second derivative of pressure with respect to y is essential for the three-dimensional dynamics, since only a balance equation for pressure with this term included can yield a realistic spatial distribution of pressure. An estimate of p_{yy} can be obtained by the assumption that the pressure distribution in axially symmetrical vortices is also axially symmetric. Then the available elements of the flow, $\underset{\sim}{V}$ and $\underset{\sim}{\nabla V}$, give an opportunity to find p_{yy}. In solid symmetrical vortices the curvature part of vorticity, VC, is much greater than the deformation, def $\underset{\sim}{V}$, and the ratio,

$$q = \frac{VC}{VC + \text{def } \underset{\sim}{V}}$$

gives a measure of the part of the flow that can be represented by a solid vortex. This ratio is approximately one when solid, completely symmetrical vortices prevail. Here def $\underset{\sim}{V}$ is the familiar three-dimensional deformation of the flow.

$$\text{def } \underset{\sim}{V} = \left[2(u_x^2 + v_y^2 + w_z^2) + (u_y + v_x)^2 + (u_z + w_x)^2 + (v_z + w_y)^2 \right]^{1/2} ,$$

and VC is the magnitude of the velocity vector multiplied by the magnitude of the three-dimensional streamline curvature vector given

in (42). On the basis of symmetry considerations, p_{yy} is estimated as

$$p_{yy} = (p_{xx}^2 + p_{zz}^2)^{1/2} \frac{VC}{VC + \text{def } V} \cos \alpha \qquad (44)$$

where α is the angle between the computing plane and the axis of rotation of the vortex. This estimate is realistic as can be seen from the examples shown in Fig. 2. For the case shown in Fig. 2(a), p_{xx} equals p_{zz}, and p_{yy} equals zero since the cos 90^o equals zero, for case 2(b), p_{zz} equals zero, and p_{xx} equals p_{yy}. In Fig. 2(c), the general case is given where p_{yy} is defined by (44). In (44) the square root of the quantity in parentheses indicates p_{yy} will be about equal to the larger of p_{xx} or p_{zz}. Therefore, the sign of p_{yy} will be made the same as that of either p_{xx} or p_{zz} depending upon which quantity has the largest absolute value. The cos α may be calculated using

$$\cos \alpha = \left(\frac{\xi^2+\zeta^2}{\xi^2+\eta^2+\zeta^2}\right)^{1/2} \qquad (45)$$

where ξ, η, and ζ are the components of the rotation vector

$$\underset{\sim}{V} \times \underset{\sim}{C} = 1/V^2 \, \underset{\sim}{V} \times \underset{\sim}{A}(\underset{\sim}{V}).$$

With the use of (44) and (45), the balance equation for pressure, (13) may now be written as

$$p_{xx}+p_{zz} = \text{div}\left[-\underset{\sim}{A}(\underset{\sim}{V})+\underset{\sim}{F}+bk\right] - \left[(p_{xx}^2+p_{zz}^2)^{1/2} \frac{VC}{VC+\text{def } V} \underset{\sim}{V} \left(\frac{\xi^2+\zeta^2}{\xi^2+\eta^2+\zeta^2}\right)^{1/2}\right]$$

In summary, the necessary assumptions so that the y derivatives may be included in this pseudo three-dimensional model are (14)-(18),

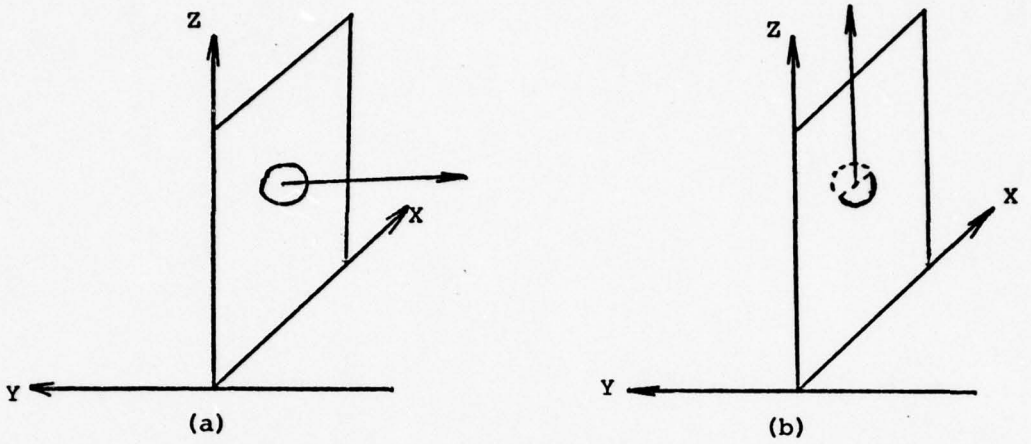

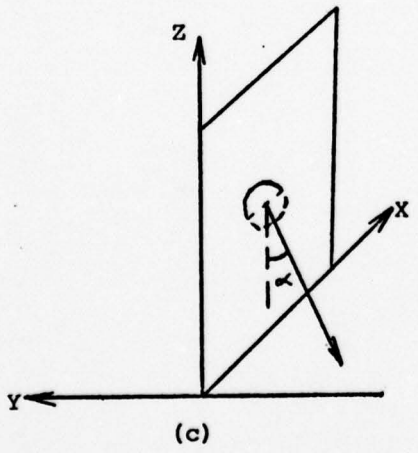

Fig. 2. Examples of the various positions of the rotation vector with respect to the xz plane. Case (a) is perpendicular, case (b) is parallel, and case (c) is at angle α (After Jenkins, 1976).

(28), (30), (43), (44), and the assumption for $(K_m u_y)_y$. With these assumptions, the basic equations can be solved step by step in time to obtain u, v, w, and b.

After the y derivatives have been introduced in the described way, it may be useful to give an explanation of the particular choice of the formulation of buoyancy in this model. The reason is that here the continuity equation does not ensure that the vertical mass flux in the updrafts is matched by the downward flux between the thermals. The continuity equation is here identically satisfied and the continuity of mass must be controlled by the formulation of buoyancy. If the buoyancy is defined as a deviation from a constant value, difficulties appear, as was experienced in preliminary computations. In such a case it depends on the choice of initial conditions how w develops. In these experiments an unstable stratification is used initially. Then the model automatically assumes that the lower regions are warmer than the adjacent regions in the y direction. Also, the upper regions are assumed colder than their laterally adjacent regions in the y direction. The consequence is that all lower regions acquire a positive vertical acceleration and the upper regions a negative one. The flow develops the physically uninteresting situation where whole horizontal belts within the plane of computation arise, while other belts sink.

Therefore, in order to simulate ascending and descending thermals side by side, the deviation from the horizontal average is used as buoyancy in (3). In this way one actually uses the classical parcel

method, where the buoyancy is proportional to the difference in temperature between the parcel and its horizontally adjacent environment, not the total environment (See Haltiner and Martin, 1957, Eqs. 5-5,5-6).

One final assumption used in this research is that the values of u, w, b, u_y, w_y, and b_y in the computational xz plane are near the maximum or minimum values with respect to the y direction. When compared to Deardorff (1965), this is a less restrictive assumption. He assumed that the values in the computational plane were the maximum or minimum values. It was found through a number of test runs that if the full y advection into the computational plane is used the values in the v field increase significantly more with time than the values in the u field. These large v values then dominate all the other variables in the various equations. However, if the magnitudes of the y advection terms in (1), (3), (4), and (15a)-(15c) are decreased to one-half their original value, this does not occur. This decrease is quite reasonable if the magnitude of the variable is already near a maximum or minimum, because one would not expect a large amount of advection. Therefore if the advection is large it should be decreased, and a decrease of one-half was found to be most beneficial.

4. NUMERICAL CONSIDERATIONS

The numerical calculation of convective flow is a rather sensitive process since an elliptic equation with von Neumann boundary conditions must be solved at each time step. To handle this an interlaced arrangement of grid points is used. The field of computation is divided into computational boxes with the grid points of pressure in the middle of each box and the velocity components in the middle of the sides normal to the respective velocity components. Since all calculations are done in the xz plane, this scheme leaves v in the same points as pressure. The buoyancy is given in the same points as w so that vertical accelerations can be evaluated with the simplest centered differences. The sides of the computational boxes are $\Delta x = \Delta z = 40$ m, so that the distance between the nearest grid points is 20 m and the distance between the nearest grid points with the same variable is 40 m. Fig. 3 shows this staggered grid arrangement. All results presented here are done in a field of 20 x 20 computational boxes.

The time extrapolation is done using the Adams-Bashforth scheme, which is

$$U^{n+1} = U^n + \Delta t \left[\frac{3}{2} \left(\frac{\partial U}{\partial t} \right)^n - \frac{1}{2} \left(\frac{\partial U}{\partial t} \right)^{n-1} \right] .$$

The time step is variable and is chosen automatically each step. The length of the time step varies accordingly to the Courant-Friedrichs-Lewy criterion for the advection terms or the von Neumann criterion derived for the diffusion terms. These criteria are given by

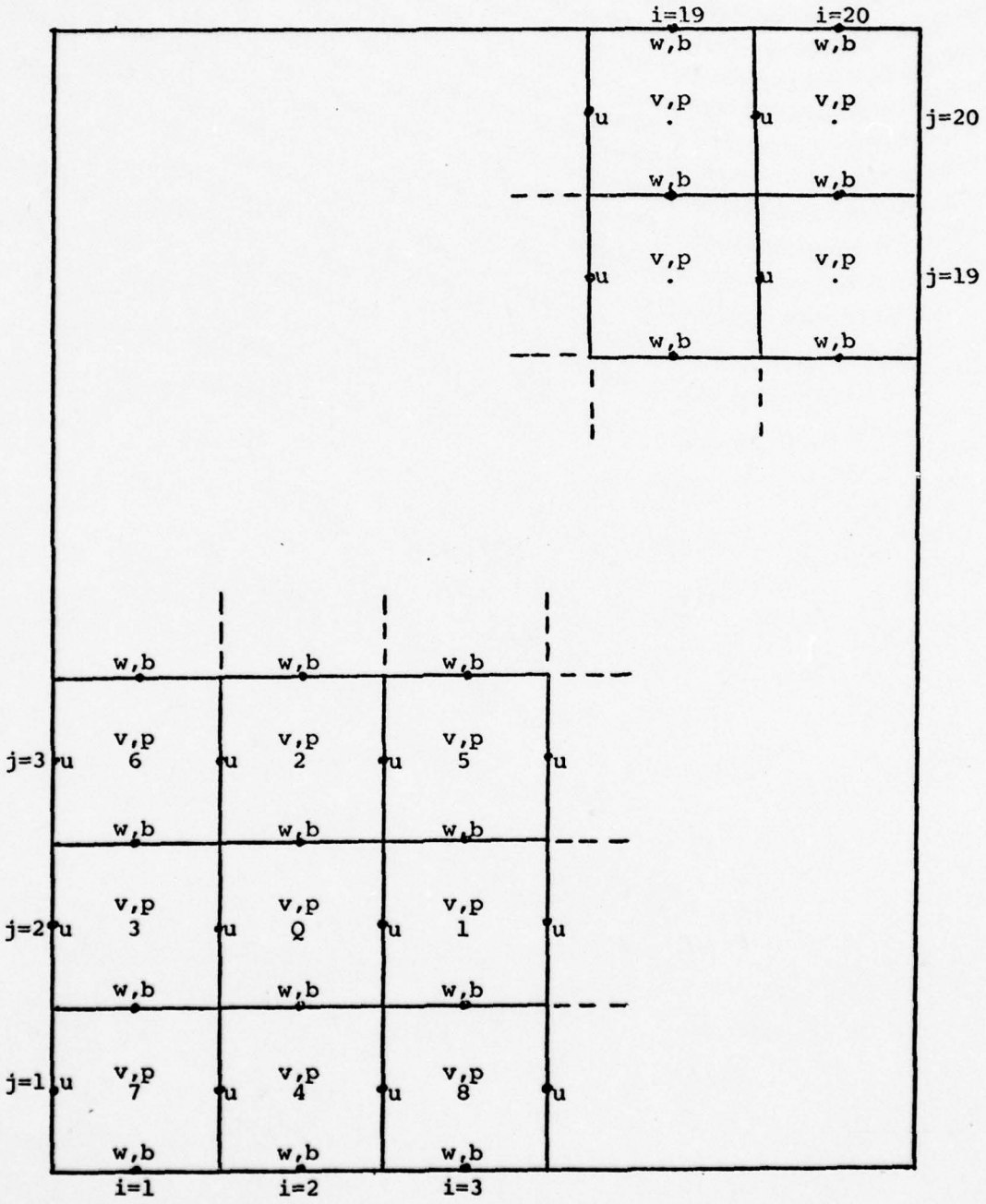

Fig. 3. Interlaced arrangement of grid points.

$$\Delta t \leq \frac{\Delta}{(u^2+v^2+w^2)^{1/2}}$$

and

$$\Delta t \leq \frac{\Delta^2}{4K_h}$$

respectively, where $\Delta = \Delta x = \Delta z$.

Spatial derivatives are approximated by upstream differences for advective terms and centered differences for diffusion terms. When centered differences are used for the advective terms, as Jenkins (1976) did, large alternating temperature gradients are found near the bottom of the model which were caused by the colder air in the descending currents and the constant temperature surface. These gradients persist due to the centered differencing scheme. When the upstream differencing scheme is used, these alternating gradients do not appear.

As an example, the finite difference formula for the advection of the u-component of velocity is shown here as

$$\begin{aligned} A(u_Q) = &- \left[\frac{u_1 + 2u_Q - u_3}{4} \left(\frac{u_Q - u_3}{\Delta x} \right) \right] \\ &- \left[\frac{v_Q + v_3}{2} (u_{yQ}) \right] \\ &- \left[\frac{w_Q + w_2 + w_3 + w_6}{4} \left(\frac{u_Q - u_4}{\Delta z} \right) \right] \end{aligned} \qquad (46)$$

for the case where u and w are positive. The averaged quantities

$$(v_Q + v_3)/2 \qquad \text{and} \qquad (w_Q + w_2 + w_3 + w_6)/4$$

are specified this way due to the staggered grid arrangement, whereas the average of

$$(u_1 + 2u_Q + u_3)/4$$

is necessary to prevent non-linear numerical instability.

The lateral boundary conditions are periodic in x, and a solid, frictional lower boundary and a solid, free-slip top boundary are assumed. The boundary conditions for the lower and upper boundaries are given by

$$u = v = w = w_y = u_y = 0 \qquad \text{at } z = 0$$

and

$$w = b_z = u_z = v_z = w_y = (u_y)_z = 0 \qquad \text{at } z = z_{top} \ .$$

Harlow and Welch (1965) show that for a frictional boundary the normal velocity at the first grid point below the boundary should be equal in both magnitude and direction to the normal velocity at the first grid point above the boundary. On the other hand, the tangential velocities below a frictional boundary should be equal in magnitude but opposite in direction to the tangential components directly above the boundary. For a free-slip boundary the normal velocity component directly above the boundary should be equal in

magnitude but opposite in direction to the normal component directly below the boundary. The tangential velocity vectors on either side of a free-slip boundary should be equal. These requirements are enforced in this model.

The initial fields of u, v, and w are set equal to zero, and then they are overlaid with a perturbation field generated by a random number program. This random number program provides a set of numbers for each level whose mean is zero and whose range is ± 0.1 m s^{-1}.

The initial potential temperature field is obtained by setting the surface potential temperature to 280.2 K, and then by decreasing the potential temperature at a rate of 2.5 K km^{-1} for the first seventeen vertical grid intervals or to a height of 680 m. Then from 680 m to 800 m, the potential temperature is increased at a rate of 25 K km^{-1}. This simulates an unstable layer beneath a very stable layer. This field is then overlaid with a perturbation field with a mean of zero and a range of ± 0.1 K for each layer. Along the bottom layer, which represents the surface, the temperatures are not permitted to change. This procedure allows localized hot areas at the surface to persist which initiate and maintain the convective thermals.

For u_y, w_y, T_y, u_{yy}, w_{yy}, and T_{yy}, where T is potential temperature, the initial fields are determined in the following manner. These fields are first set equal to zero, and then they are overlaid with a perturbation field generated by a random number program. This program provides a set of numbers for each level whose mean is zero.

The range of the random numbers at each level is

$$\pm \left[\overline{(v_x)^2}^x \right]^{1/2} \quad \text{for } u_y$$

$$\pm \left[\overline{(w_x)^2}^x \right]^{1/2} \quad \text{for } w_y$$

$$\pm \left[\overline{(T_x)^2}^x \right]^{1/2} \quad \text{for } T_y$$

$$\pm \left[\overline{(v_{yx})^2}^x \right]^{1/2} \quad \text{for } u_{yy}$$

$$\pm \left[\overline{(w_{yx})^2}^x \right]^{1/2} \quad \text{for } w_{yy}$$

$$\pm \left[\overline{(T_{yx})^2}^x \right]^{1/2} \quad \text{for } T_{yy} \; .$$

The numerical procedure was tested for numerical stability using a small 3 X 3 grid network over an extended time period. This represents a very severe test since there are eight boundary points and only one interior point. The test, which ran for 1000 time steps representing slightly over two hours of simulated time, demonstrated that the numerical solution is stable.

5. RESULTS

The computer program of this model is constructed for the pseudo three-dimensional model, hereafter referred to as 3D, described earlier. However, if one variable is changed in this program, all of the y derivatives are set equal to zero and the result is a two-dimensional slab-symmetric model denoted here by 2D. This is done so that the two models have the same initial and boundary conditions. This allows direct comparisons to be made between the 2D and 3D cases. These comparisons are shown in Figs. 4-16.

Figs. 4 and 5 show the vertical velocity and potential temperature deviation fields for the 2D case after approximately 5 min of simulated time. Figs. 6 and 7 show the same fields for the 3D case at a similar time. The corresponding diagrams for the 2D and 3D models are very much alike. However upon close scrutiny, one can see that the 3D case (Fig. 6) is slightly farther along in development than the 2D case in Fig. 4 when both are compared to what occurs at a later time. The secondary thermal at (19,6) which will dissipate in later time steps, has a smaller vertical velocity, 0.238 m s^{-1}, in the 3D case compared to 0.418 m s^{-1} in the 2D model. The downdraft at (11,5) in Fig. 6 which will also dissipate later, has a minimum vertical velocity of -0.309 m s^{-1}, compared to a value of -0.359 m s^{-1} in the downdraft at (11,6) in Fig. 4. The maximum w in the whole field is 0.875 m s^{-1} in the 3D model and only 0.824 m s^{-1} for the 2D case. At about 10 min of simulated time, Figs. 8-11, the difference between the two cases is more apparent. The maximum

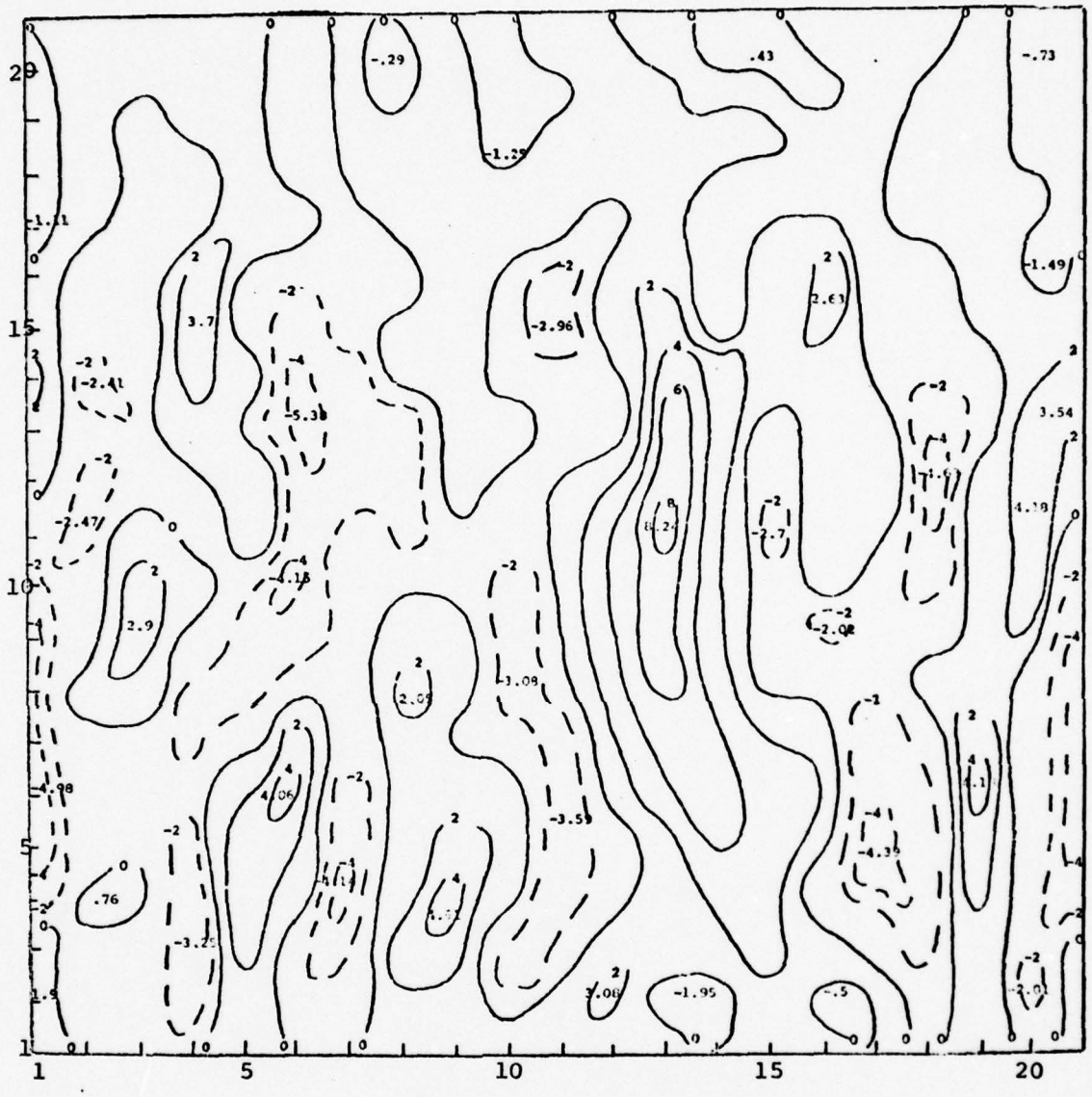

Fig. 4. 2D vertical velocity (10^{-1} m s^{-1}) at 4 min 46 s. Positive values are represented by solid lines, while negative values are shown by dashed lines. The tick marks and numbers in this figure and the succeeding ones along the left hand side and the bottom show the position of the vertical and horizontal grid points, respectively.

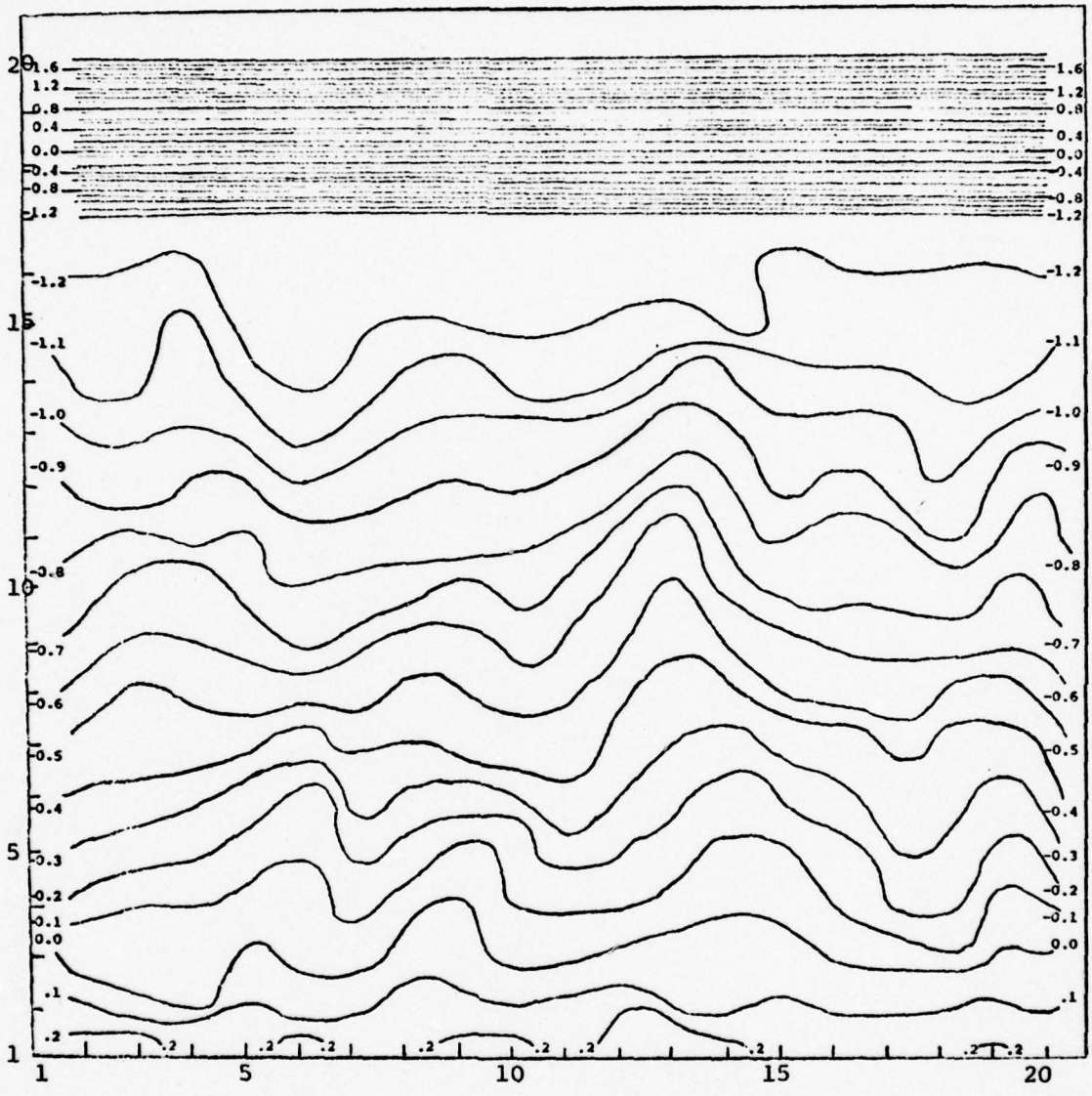

Fig. 5. 2D potential temperature deviation (10^{-1} K) from 280 K at 4 min 46 s.

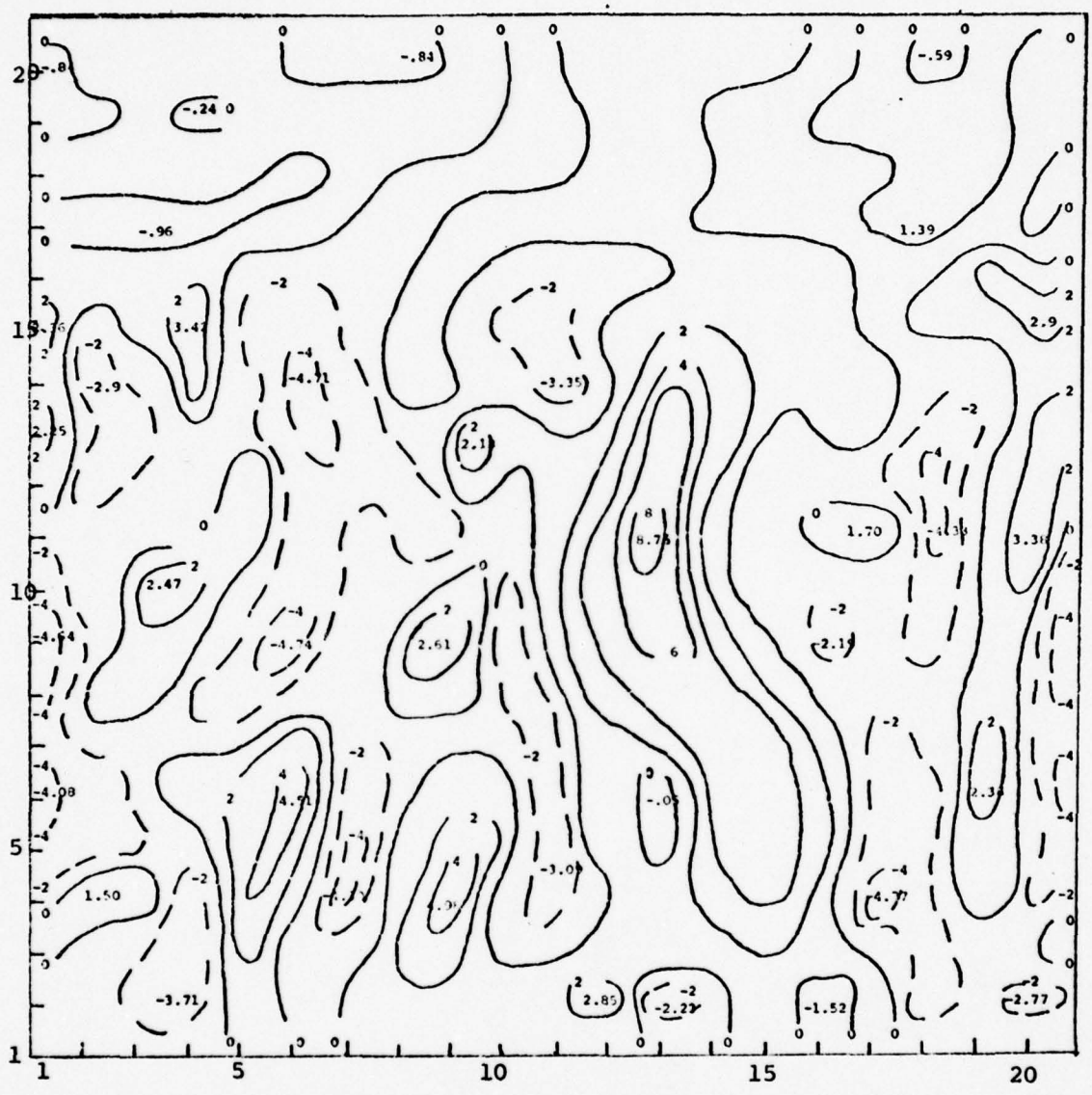

Fig. 6. 3D vertical velocity (10^{-1} m s^{-1}) at 4 min 42 s.

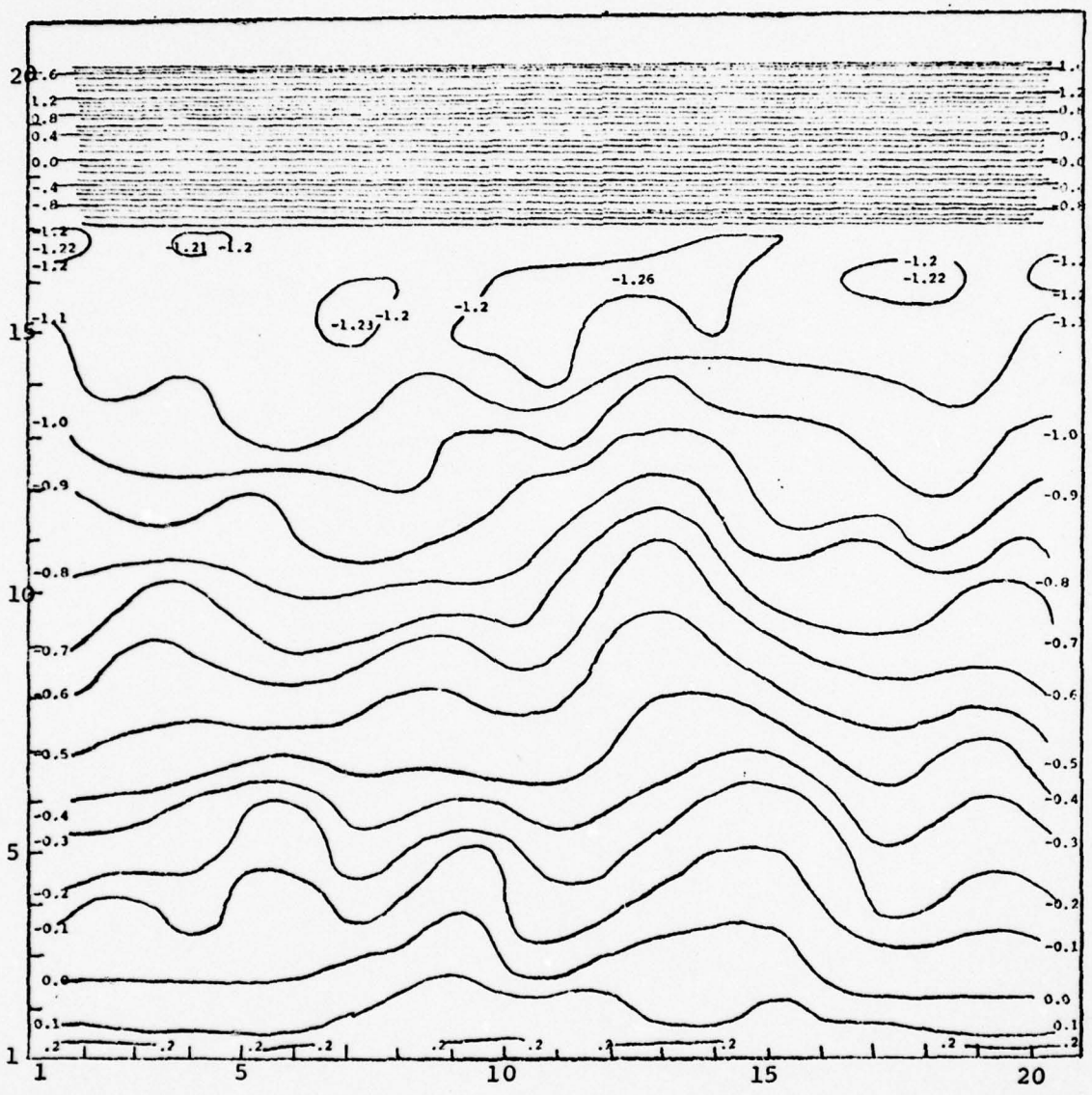

Fig. 7. 3D potential temperature deviation (10^{-1} K) from 280 K at 4 min 42 s.

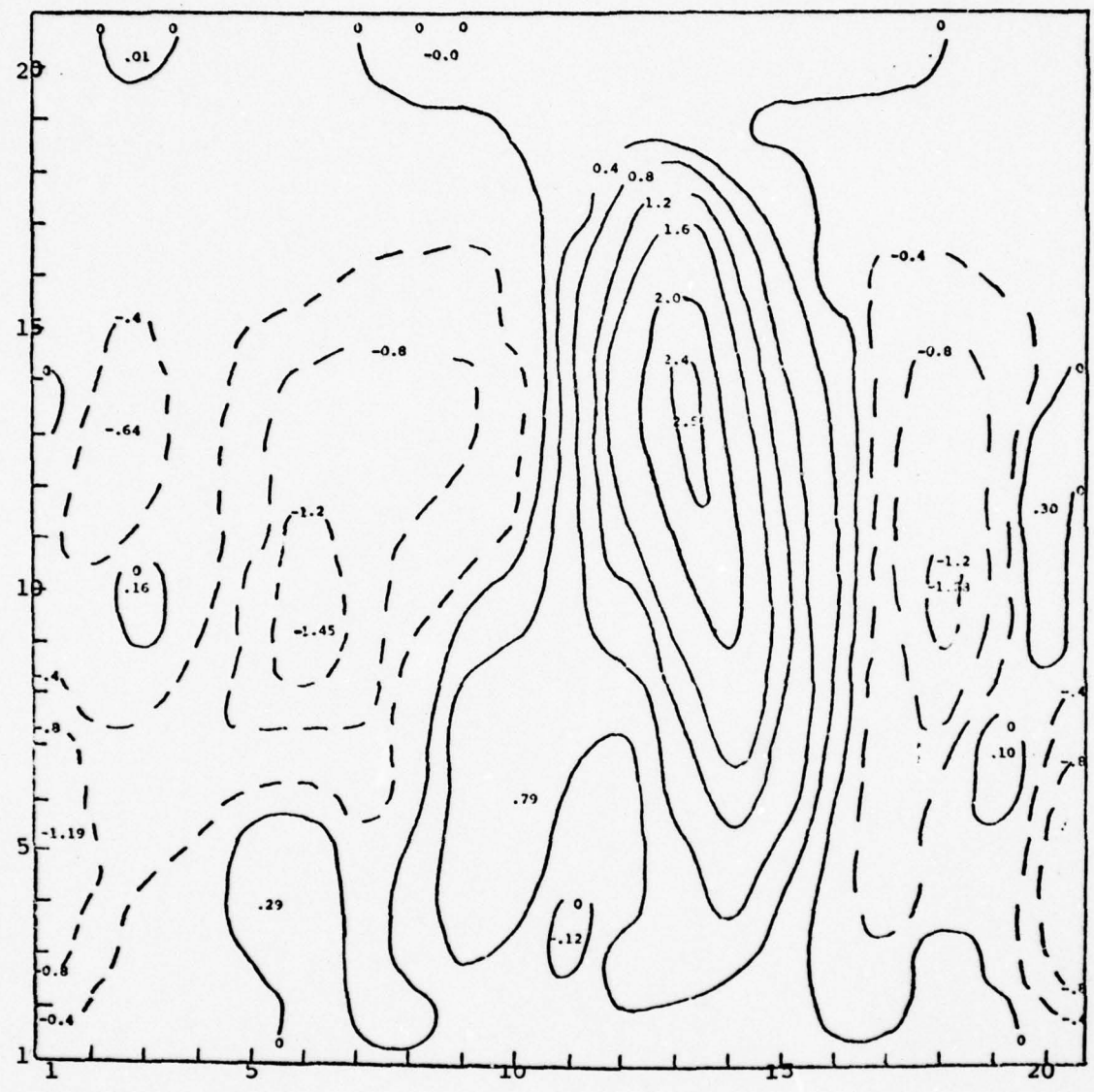

Fig. 8. 2D vertical velocity (m s^{-1}) at 10 min 52 s.

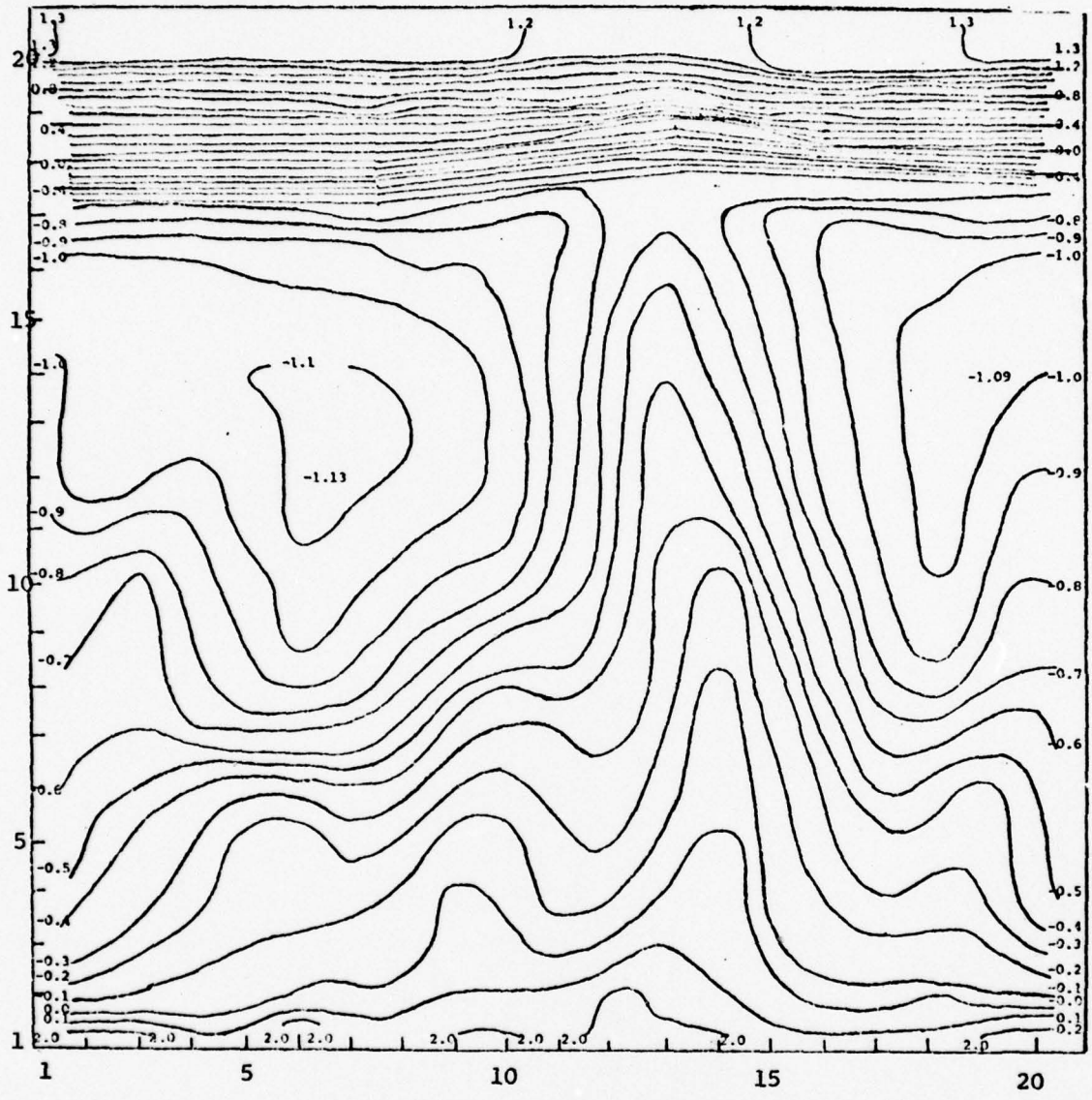

Fig. 9. 2D potential temperature deviation (10^{-1} K) from 280 K at 10 min 52 s.

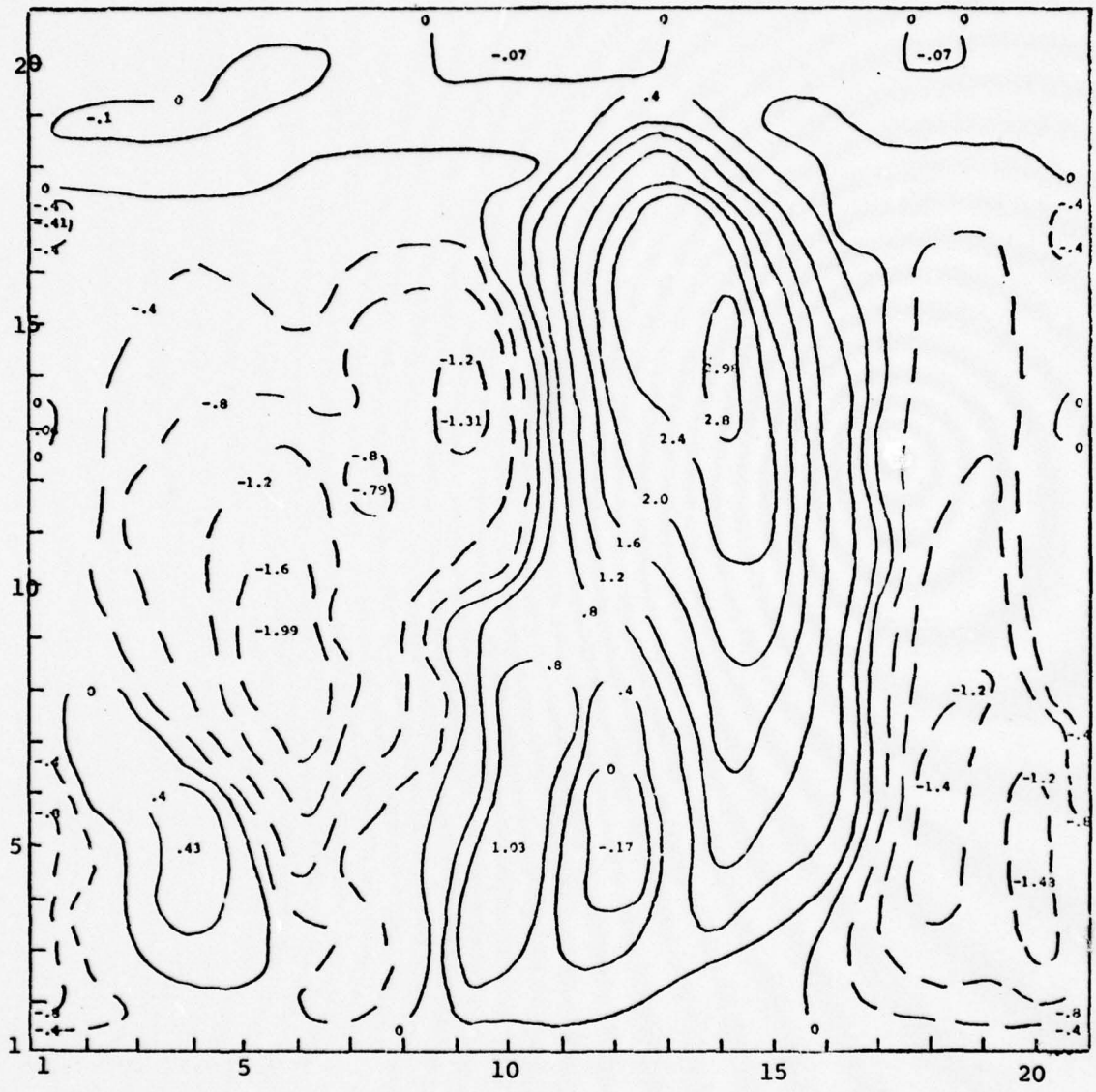

Fig. 10. 3D vertical velocity (m s^{-1}) at 10 min 27 s.

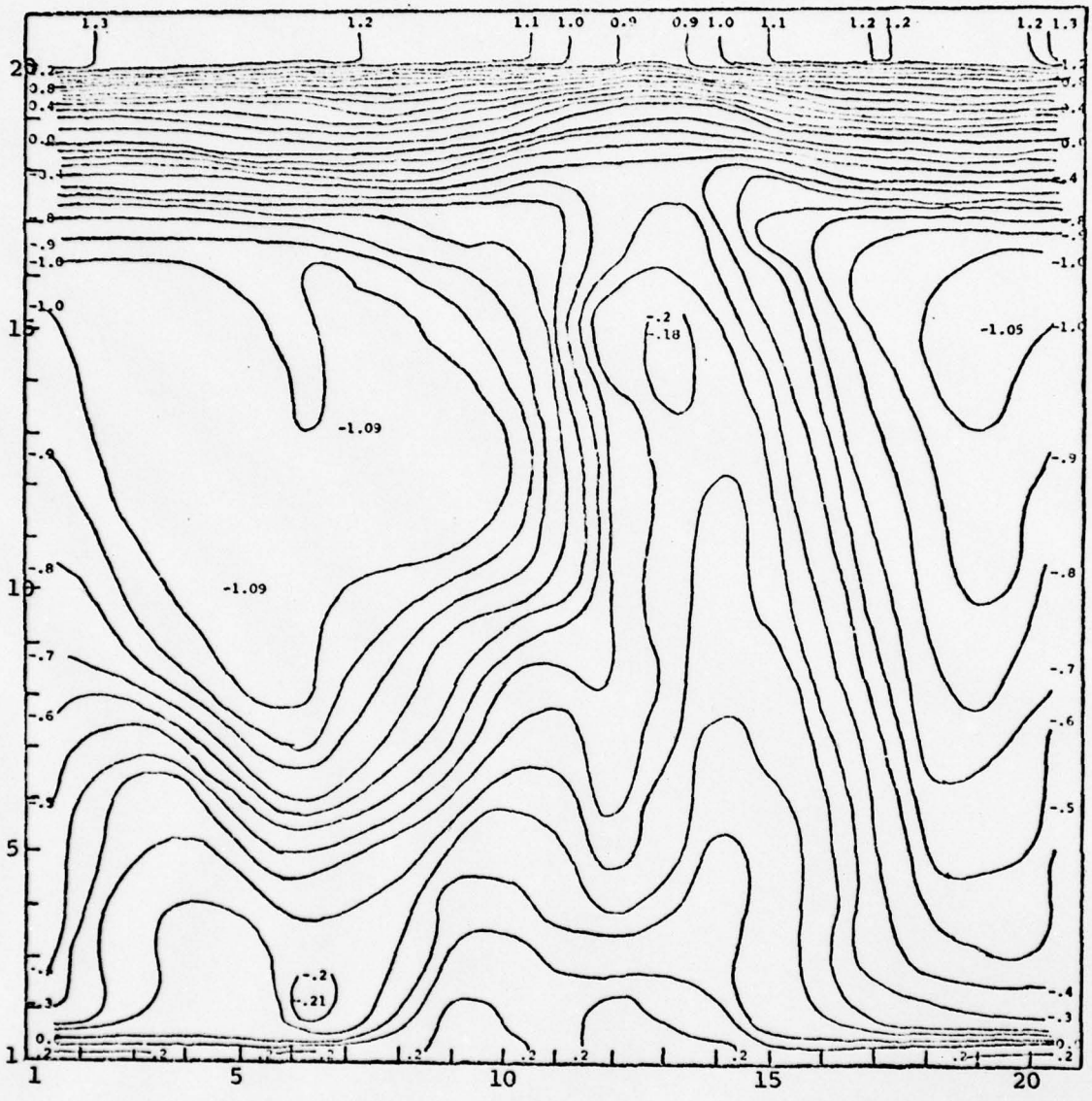

Fig. 11. 3D potential temperature deviation (10^{-1} K) from 280 K at 10 min 27 s.

w for the 3D model is 17% larger and 80 m higher than that for the 2D model. A secondary thermal at horizontal grid point 4 in Fig. 10 is better organized with a maximum w of 0.43 m s^{-1} in the 3D case compared to 0.29 m s^{-1} in the 2D case. The downdrafts are also farther along in development. The minimum w in the downdraft at horizontal grid point 18 in Fig. 10 is smaller and 160 m lower than that for the 2D case. The major difference in the potential temperature deviation fields at this time between the two models is that warmer air is carried to a greater height in the 3D case. In Fig. 11, a value of -0.18 K reaches the 600 m level compared to 400 m level for the 2D case. Continuing in time, Figs. 12-15 show the two fields for the 2D and 3D cases at about 15 min, which for the 2D case is the time of maximum development. For the 2D model there are one updraft and two downdrafts giving a transverse roll circulation. These rolls with their axes normal to the plane of the model are similar to the circulation patterns that Steiner (1973) found with his slab-symmetric model. He stated that these rolls would not necessarily occur if three-dimensional circulation was possible. This is confirmed in the computed 3D case, since the roll circulation is greatly modified. The vertical motion and the potential temperature deviation in Figs. 14 and 15 show signs of being influenced from outside the computational plane. This is especially noticeable for the two updrafts, one at (1,6) and another at (6,12). These updrafts were initiated by warm air advection into these areas from the simulated y direction. Likewise, cold advection

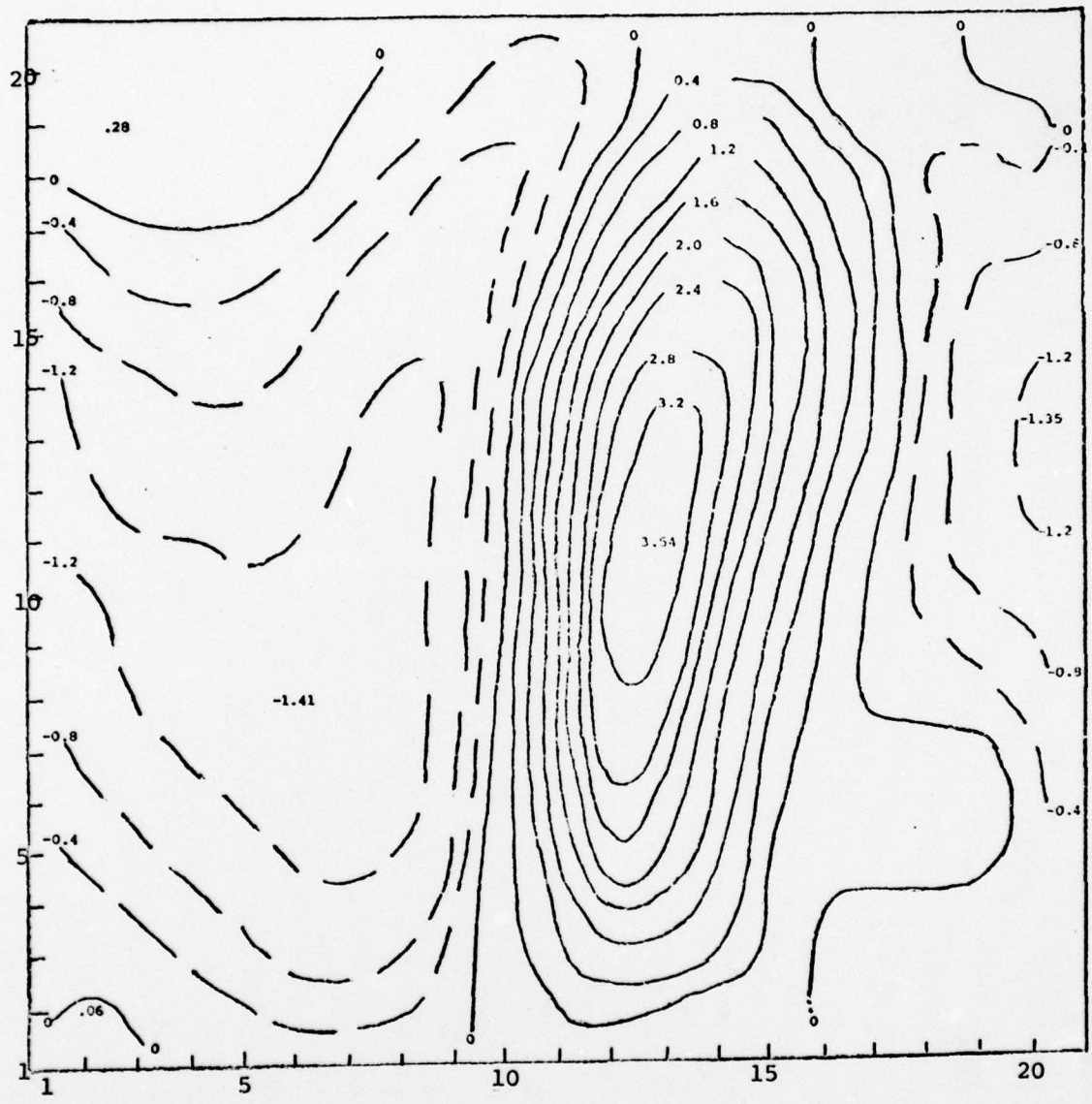

Fig. 12. 2D vertical velocity (m s^{-1}) at 15 min 19 s.

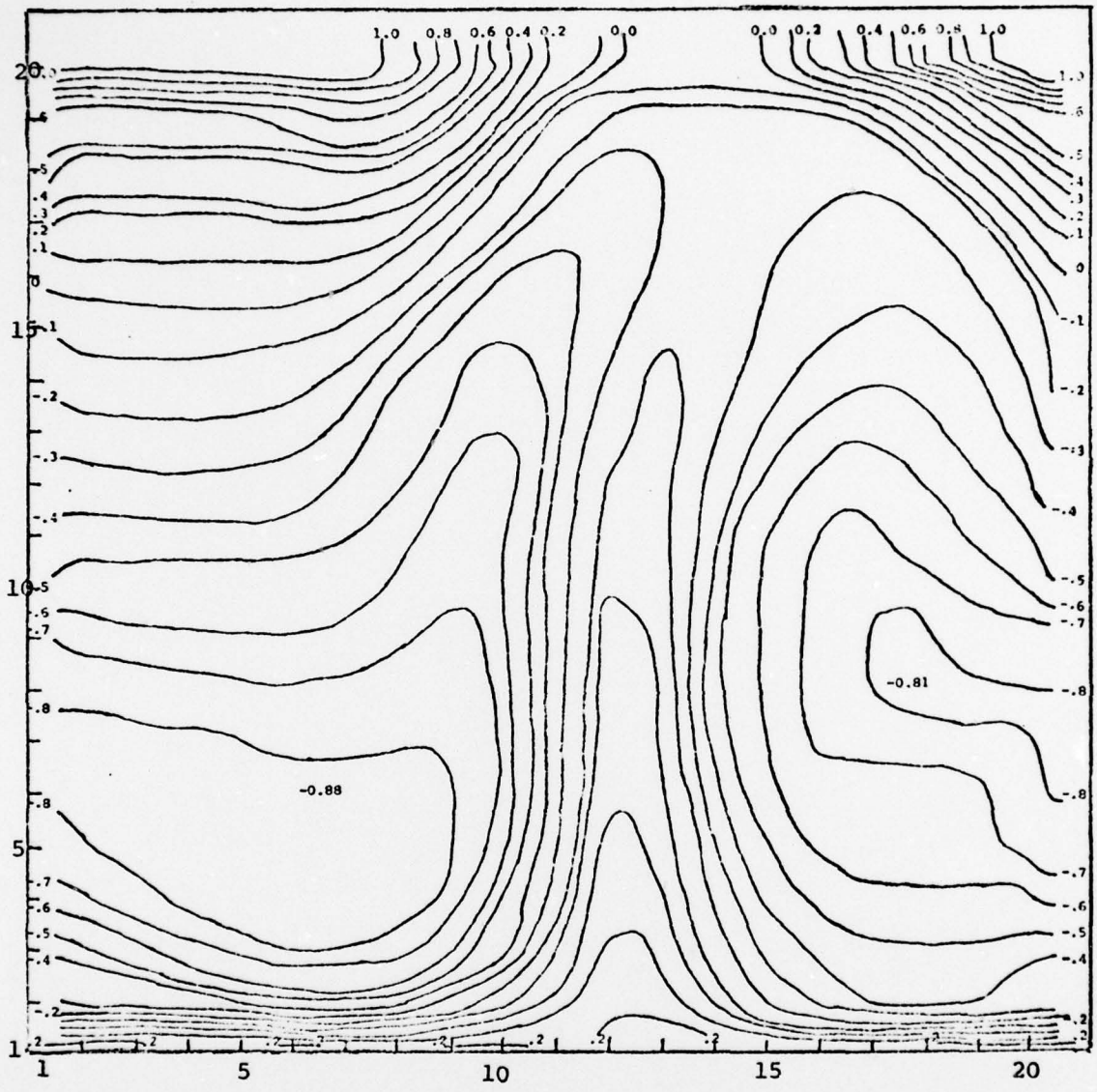

Fig. 13. 2D potential temperature deviation (10^{-1} K) from 280 K at 15 min 19 s.

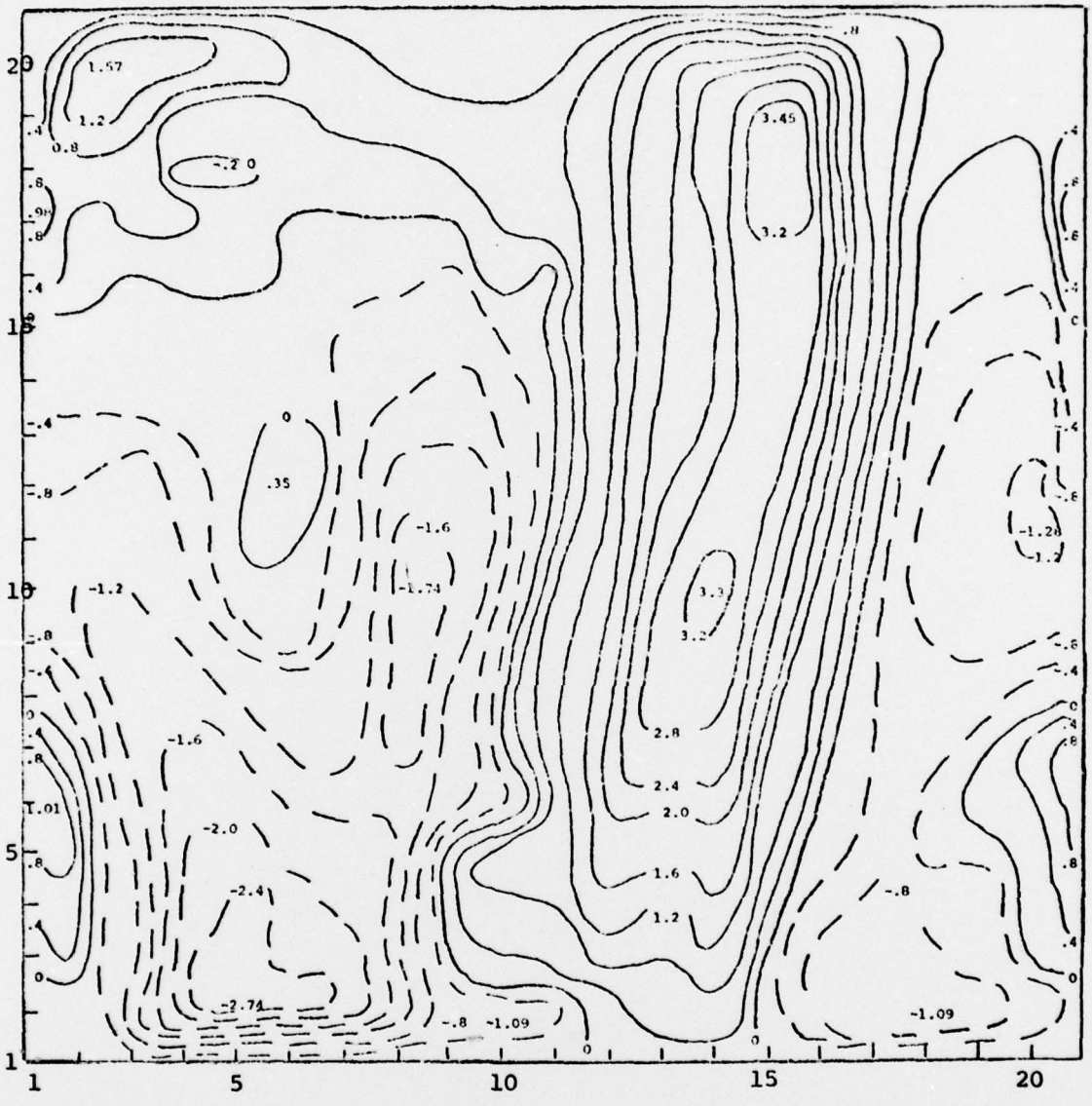

Fig. 14. 3D vertical velocity (m s^{-1}) at 15 min 24 s.

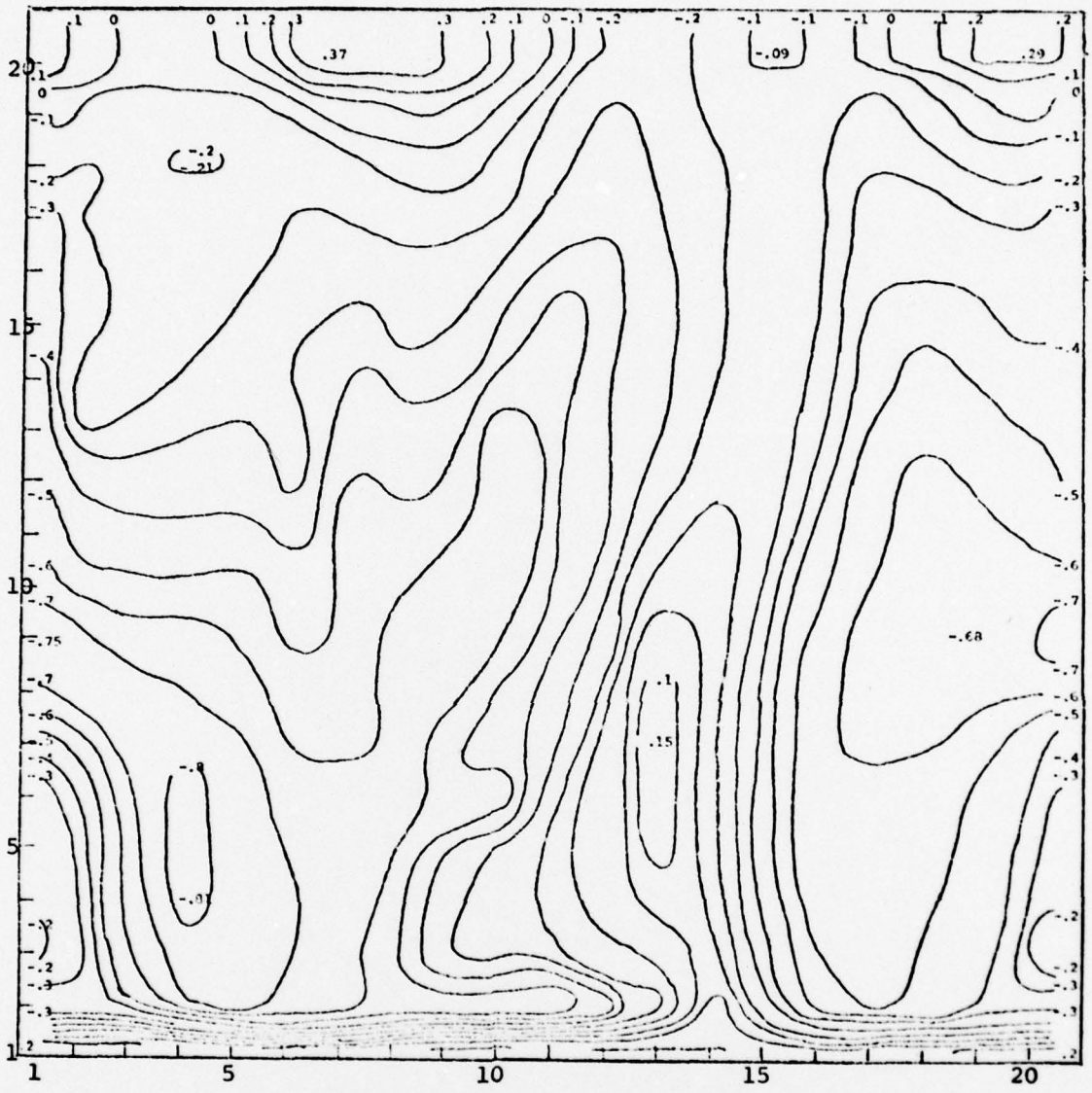

Fig. 15. 3D potential temperature deviation (10^{-1} K) from 280 K at 15 min 24 s.

from the simulated y direction near the bottom of the model has enhanced the two downdrafts at (5,1) and (18,1). Another noteworthy feature of Fig. 14 is the secondary maximum that does not appear in Fig. 12. Soong and Ogura (1973) found a similar secondary maximum in their axisymmetric model which did not appear in the slab-symmetric model used for comparison.

The time variation of the maximum w values at each time step are given for the 2D and 3D models in Fig. 16. After 2 min of simulated time, the 3D maximum w values are larger than those of the 2D model, except for a brief period between 15 and 16 min. The maximum difference occurs at 12.7 min when the 2D maximum w is only 0.82 of the maximum w in the 3D model. In order to compare the two models, the ratio of the maximum w for the 2D model for the entire time period to that of the 3D model is formed. In this research the ratio is 0.90, while similar ratios found by other investigators who have compared two- and three-dimensional models are 0.71 by Wilhelmson (1972), 0.35 by Steiner (1973), and 0.51 by Wilhelmson (1974). Although these values are quite different, they affirm that the three-dimensional maximum w is always larger than the two-dimensional case in similar circumstances. Fig. 16 also shows that the maximum w, besides being larger, occurs sooner. In the 3D case the maximum w occurs at 12.7 min with secondary maximums at 14.8 and 16.4 min. In contrast, the maximum w in the 2D model is not reached until 15 min with secondary maximums at 12 and 16 min. Therefore the 2D model takes 18% more time to reach its maximum than

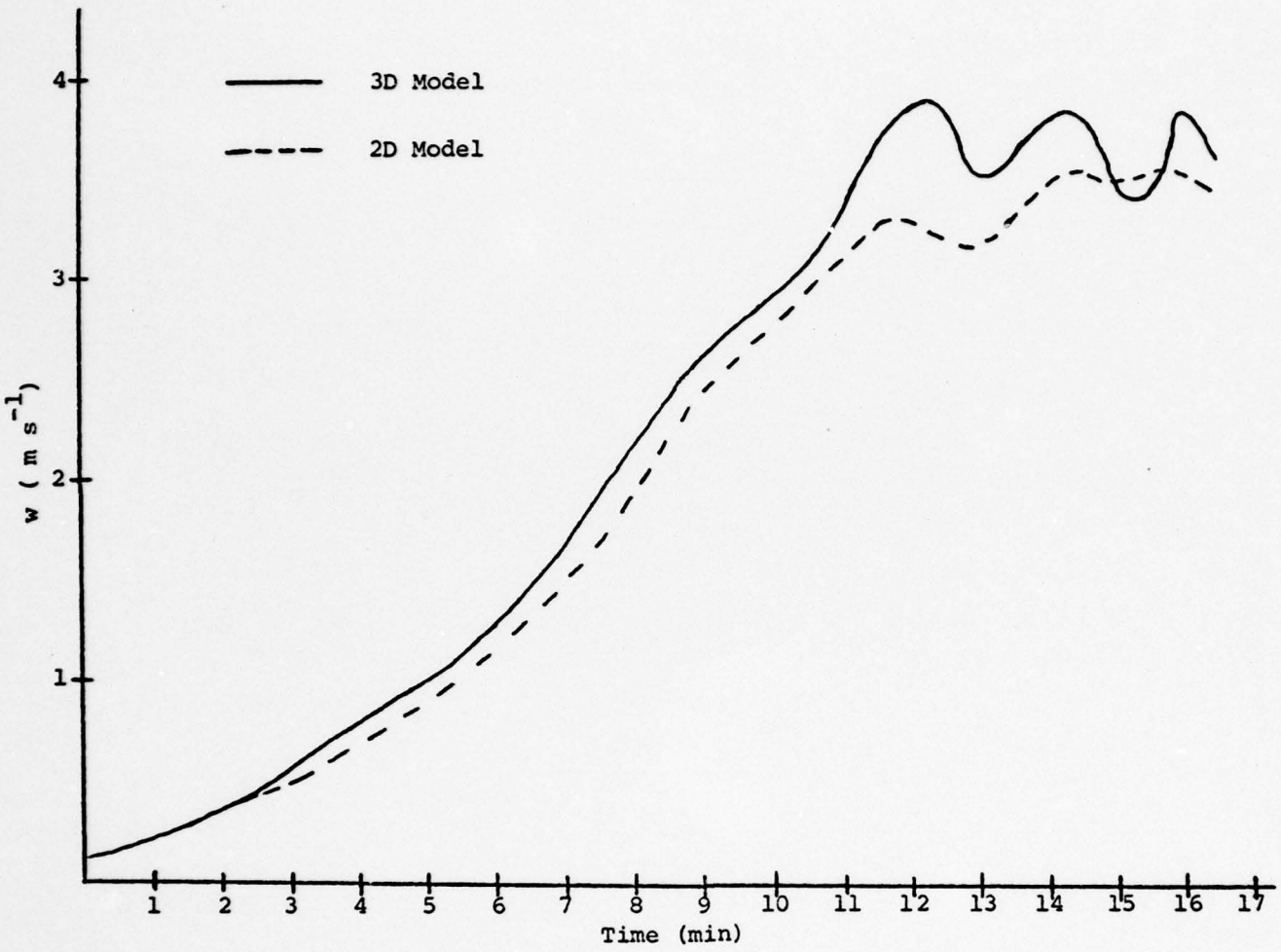

Fig. 16. Time variation of maximum vertical velocity for 3D and 2D models.

the 3D case. This is in good agreement with other researchers who have made similar comparison of this time difference. They have found values of 22% (Wilhelmson, 1974), 7% (Steiner, 1973), and 13% (Soong and Ogura, 1973).

Another comparison that can be made between the 2D and 3D models is the rate of ascent for maximum w. The level of maximum w for the 2D case rises at 0.50 m s^{-1} while for the 3D case the ascent is 0.73 m s^{-1}. The ratio of the 3D case to that of the 2D is 1.46. This can then be related to the researchers' work mentioned before. Soong and Ogura (1973) found the rate of ascent for the axisymmetric to be 2.24 m s^{-1}, while the rate for their slab-symmetric model was 1.52 m s^{-1}. The ratio of these two is 1.47. Wilhelmson (1974) found a similar ratio of 1.78. The lack of uniformity among the rates of ascent among the various researchers could be contributed to the different initial or boundary conditions, whether moisture was accounted for and in what way it was handled if it was included, or different lapse rates. However the important part in the comparison of the 2D and 3D models is the ratio of the ascent rates, and the ratio found in this research compares favorably with others.

From these comparisons, one can see that the 3D thermals grow faster, have a larger vertical motion, and reach this larger w value faster than the thermals in the 2D case. Also the unlikely transverse roll circulation formed in the 2D case is greatly modified in the 3D model.

6. CONCLUSION

The aim of this study was to show the possibility of including the y derivatives in a two-dimensional model of convection in such a way that a simulation of the three-dimensional flow is achieved. The necessary y derivatives were included by assuming:

(a) horizontal isotropy of derivatives for u_y, w_y, b_y, u_{yy}, w_{yy}, and b_{yy},

(b) quasi-cyclostropic balance for p_y, and

(c) symmetry of solid vortices for p_{yy}.

By assuming horizontal isotropy of derivatives, additional constraints arise so that the simulated y advection does not affect the mean or the mean squared values. Jenkins (1976) failed to constrain these terms, and he experienced numerical stability problems. After these constraints were enforced in this research, the numerical solution was stable.

The results of this research are quite encouraging and demonstrated that the two-dimensional assumptions may be improved by pseudo three-dimensional assumptions to produce thermal convection in better agreement with true three-dimensional models. However certain limitations need further investigation. The vertical gradient of the vertical velocity is stronger above the velocity maximum than below it. This is probably due to insufficient mixing in the model in this area. Also it is found that the v value directly above the maximum w is much smaller than the surrounding values which restricts the y advection terms there. From a number of other experiments, these

two limitations have been shown to cause a slower ascent rate and an overall smaller maximum w than other researchers have found. These two limitations are possibly connected since v_y is determined by the continuity equation in which w_z is a major term.

Another limitation is that no lateral spreading of the thermals occur as they rise. Steiner (1973) reports a similar finding. He felt there was insufficient dissipation and increased the value of c which is used in the calculation of the eddy viscosity coefficient to 0.42. This value or one between the present value used and 0.43 should be tested. Experimental research is also needed to determine why the ratio of minimum to maximum w in this model is larger than those values reported by investigators of three-dimensional models. The smaller y advection term in the vicinity of w maximum mentioned previously may be the cause of this.

When the preceeding limitations are resolved, moisture may then be added and the model extended to the study of convection which is not horizontally isotropic. This extension would require the introduction of empirical constants differing slightly from unity which will relate the y derivatives to the x derivatives.

Should the simulation of atmospheric convection be successful using a pseudo three-dimensional model, more researchers will be able to investigate this process more fully with the computer facilities readily available to them.

REFERENCES

Blair, A., N. Metropolis, J. von Neumann, A.H. Taub, and M. Tsingou, 1959: The evolution of a convective element: A numerical calculation. The Atmosphere and the Sea In Motion, New York, Rockefeller Institute Press, 425-439.

Deardorff, J.W., 1965: A numerical study of pseudo three-dimensional parallel plate convection. J. Atmos. Sci., 22, 419-435.

———, 1970: A numerical study of three-dimensional turbulent channel flow at large Reynolds numbers. J. Fluid Mech., 41, 453-480.

———, 1971: On the magnitude of the subgrid scale eddy coefficient. J. Comp. Physics, 7, 120-133.

———, 1972: Numerical investigation of neutral and unstable planetary boundary layers. J. Atmos. Sci., 29, 91-115.

———, 1973: The use of subgrid transport equations in a three-dimensional model of atmospheric turbulence. J. Fluids Eng., 95, 429-483.

Fox, P.G., 1972: Numerical simulation of three-dimensional, shape preserving convection elements. J. Atmos. Sci., 29, 322-341.

Gruneberg, W., 1975: Ein zweidimensionales numerisches Konvektionsmodell mit dreidimensionaler Dynamik. Master's thesis, Institut fur Meteorologie, Freie Universitat, Berlin.

Haltiner, G.J., and F.L. Martin, 1957: Dynamical and Physical Meteorology, New York, McGraw-Hill, 470 pp.

Harlow, F.H., and J.E. Welch, 1965: Numerical calculation of time-dependent viscous incompressible flow of fluid with free surface. Phys. of Fluids, 8, 2182-2189.

Hinze, J.O., 1975: Turbulence. New York, McGraw-Hill, 790 pp.

Holton, J.R., 1972: An Introduction to Dynamical Meteorology. New York, Academic Press, Inc., 319 pp.

Huschke, R.E., ed., 1959: Glossary of Meteorology. Boston, American Meteorological Society, 638 pp.

Jenkins, E.W., 1976: A pseudo three-dimensional convection model. Master's thesis, Texas A&M University.

Leith, C.C., 1965: Numerical simulation of the earth's atmosphere. Methods In Computational Physics, Vol. 4, New York, Academic Press, 1-27.

Leith, C.E., 1968: Diffusion approximations for two-dimensional turbulence. Phys. Fluids, 11, 671-674.

Lilly, D.K., 1962: On the numerical simulation of buoyant convection. Tellus, 14, 148-172.

———, 1965: On the computational stability of numerical solutions of time-dependent non-linear geophysical fluid dynamics. Mon. Wea. Rev., 93, 11-26.

Lilly, D.K., 1966: On the application of the eddy viscosity concept in the inertia subrange of turbulence. National Center for Atmospheric Research, Boulder, Colo., Manuscript No. 123.

———, 1967: The representation of small-scale turbulence in numerical simulation experiments. Proceedings of the IBM Scientific Computing Symposium on Environmental Sciences, IBM Form No. 320-1951.

Miller, M.J., and R.P. Pearce, 1974: Three-dimensional primitive equation model of cumulonimbus convection. Quart. J. Roy. Meteor. Soc., 100, 133-154.

Mintz, Y., 1965: Very long term global integration of the primitive equations of atmospheric motion, W.M.O. Technical note No. 66, W.M.O. - I.U.G.G. Symposium on Research and Development Aspect of Long Range Forecasting, 141-167.

Ogura, Y., and J.G. Charney, 1960: A numerical model of thermal convection in the atmosphere. Proc. Intern. Symp. Numerical Weather Prediction, Tokyo, Japan Meteor. Soc., 431-451.

———, 1962: Convection of isolated masses of a buoyant fluid: A numerical calculation. J. Atmos. Sci., 19, 492-502.

Orville, H.D., 1964: On mountain upslope winds. J. Atmos Sci., 21, 622-633.

———, 1965: A numerical study of the initiating of cumulus convection over mountainous terrain. J. Atmos Sci., 22, 684-699.

———, 1968: Ambient wind effects on the initiation and development of cumulus clouds over mountains. J. Atmos. Sci., 25, 385-403.

Pond, S., R.W. Stewart, and R.W. Burling, 1963: Turbulence spectra in the wind over waves. J. Atmos. Sci., 20, 319-324.

Schlesinger, R.E., 1975: A three-dimensional numerical model of an isolated deep convective cloud: Preliminary results. J. Atmos. Sci., 32, 934-957.

Scorer, R.S., and R.S. Richards, 1959: The behavior of chimney plumes. Intern. J. Air Poll., 1, 198-220.

Smagorinsky, J., 1963: General circulation experiments with primitive equations: 1. The basic experiment. Mon. Wea. Rev., 91, 97-164.

Squires, P., and J.S. Turner, 1962: An entraining jet model for cumulonimbus updraughts. Tellus, 14, 422-434.

Steiner, J.T., 1973: A three-dimensional model of cumulus cloud development. J. Atmos. Sci., 30, 414-435.

Taylor, G.I., 1935: Statistical theory of turbulence-I. Proc. Roy. Soc. A., CLI, 421-444.

Wilhelmson, R., 1972: The numerical simulation of a thunder storm cell in two- and three-dimensions. Ph.D. thesis, University of Illinois.

Wilhelmson, R., 1974: The life cycle of a thunderstorm in three dimensions. J. Atmos. Sci., 31, 1629-1651.

VITA

The author was born in Ellwood City, Pa., on April 28, 1948. His parents, Mr. and Mrs. Edward J. Weyman, reside at 429 Highland Avenue, Zelienople, Pa. 16063. This also serves as the author's permanent address.

Captain Weyman graduated from Seneca Valley High School in Harmony, Pa., and then continued his formal education at Grove City College, Grove City, Pa. It was from Grove City College that he received a Bachelor of Science degree in mathematics in 1970 and was commissioned a second lieutenant in the Air Force. Captain Weyman's first assignment was to attend a one year course in basic meteorlogy at Texas A&M University after which he was sent to Forbes Air Force Base in Topeka, Ks., as a detachment forecaster. In 1973, Captain Weyman was reassigned to Heidelberg, Germany, where he served four years as a squadron level forecaster supporting army operations in Europe. While in Germany, Captain Weyman earned a Master of Science degree in Business Administration from Metropolitan College of Boston University. He was then selected by an Air Force Institute of Technology screening board to attend Texas A&M University in order to obtain a Master of Science degree in Meteorology.

Captain Weyman is married to the former Linda J. Cunningham. They have two children, Paul Adam and Rachel Edith.

The typist for this thesis was Sue E. Hamilton, sister of the author.